Author Manuscript

Author Manuscript

Author Manuscript

Author Manuscript

HHS Public Access

Author manuscript

Sci Transl Med. Author manuscript; available in PMC 2023 August 30.

Published in final edited form as:

Sci Transl Med. 2022 May 25; 14(646): eabn4772. doi:10.1126/scitranslmed.abn4772.

Aberrant methylmalonylation underlies methylmalonic acidemia and is attenuated by an engineered sirtuin

PamelaSara E. Head[1,2], **Sangho Myung**[2], **Yong Chen**[3], **Jessica L. Schneller**[2], **Cindy Wang**[2], **Nicholas Duncan**[2], **Pauline Hoffman**[2], **David Chang**[2], **Abigael Gebremariam**[2], **Marjan Gucek**[3], **Irini Manoli**[2], **Charles P. Venditti**[2,*]

[1]National Institute of General Medical Sciences, NIH, 45 Center Drive MSC 6200 Bethesda, MD, 20892-6200 USA

[2]National Human Genome Research Institute, NIH, Bethesda, MD, 10 Center Drive Building 10, Room 7S257 Bethesda, MD 20892, USA

[3]National Heart Lung and Blood Institute, NIH, Building 31, 31 Center Drive Bethesda, MD 20892, USA

Abstract

Organic acidemias such as methylmalonic acidemia (MMA) are a group of inborn errors of metabolism that typically arise from defects in the catabolism of amino and fatty acids. Accretion of acyl-CoA species is postulated to underlie disease pathophysiology, but the mechanism(s) remain unknown. Here, we surveyed hepatic explants from patients with MMA and unaffected donors, in parallel with samples from various mouse models of methylmalonyl-CoA mutase (MMUT) deficiency. We found a widespread posttranslational modification, methylmalonylation, that inhibited enzymes in the urea cycle and glycine cleavage pathway in MMA. Biochemical studies and mouse genetics established that sirtuin 5 (SIRT5) controlled the metabolism of MMA-related posttranslational modifications. SIRT5 was engineered to resist acylation-driven inhibition via lysine to arginine mutagenesis. The modified SIRT5 was used to create an adeno-associated viral (AAV) 8 vector and systemically delivered to mutant and control mice. Gene therapy ameliorated hyperammonemia and reduced global methylmalonlyation in the MMA mice.

One Sentence Summary:

Hyperacylation, specifically methylmalonylation, underlies disease pathophysiology in MMA and can be modulated by SIRT5 activity.

*Correspondence should be addressed to C.P.V. (venditti@mail.nih.gov).

Author contributions:

PEH designed and performed the majority of experiments outlined in this manuscript and wrote the manuscript. CPV also aided in experimental design, manuscript drafting. SM performed experiments for mitochondrial DNA copy number assays in Figure 3C and 3D, assisted with murine experiments for Figures 5 and 6, and performed the hyperpropionylated SuperSIRT5 in vitro activity assay for fig S5B. YC performed mass spectrometry analysis of prepared murine liver tissue lysates. JS generated and characterized the *Mmut*$^{G715V/G715V}$ mouse line used to generate the *Sirt5*$^{-/-}$;*Mmut*$^{G715V/G715V}$ mouse line. CW and IM generated the *Acsf3*$^{-/-}$ mouse line. MG assisted in experiment design for the MMA PTM proteome analysis. PEH, ND, PH, DC, and AG performed Western blots analysis to determine Sirt/SIRT and urea cycle enzyme protein abundance in mouse and human liver tissue.

Competing Interests:

The other authors declare that they have no competing interests.

Overline: INBORN ERRORS OF METABOLISM

Author Manuscript Author Manuscript Author Manuscript Author Manuscript

Editor's summary: Methylmalonylation in metabolic disease

Methylmalonic acidemia (MMA) is a genetic metabolic disorder that results in a buildup of methylmalonic acid in the body and can lead to severe symptoms. Examining liver tissue from patients and a mouse model of MMA, Head *et al.* found that the buildup of this metabolite resulted in a widespread posttranslational modification, methylmalonylation, on a variety of proteins. This included the sirtuin (SIRT5) that reverses methylmalonylation, dampening its ability to undo the protein modification damage. A SIRT5 gene engineered to be resistant to methylmalonylation reduced symptoms in the MMA mice, demonstrating a proof of concept gene therapy strategy.

INTRODUCTION

During vertebrate metabolism, the terminal catabolism of essential amino acids (AAs) valine, isoleucine, methionine, and threonine as well as odd chain fatty acids (OCFAs) and cholesterol into the Krebs cycle intermediate succinyl-CoA is mediated by the vitamin B12 (cobalamin) dependent enzyme methylmalonyl-CoA mutase (MMUT) (1–3). A deficiency of MMUT or its obligate cofactor, 5'-deoxyadenosylcobalamin (AdoCbl) results in the accretion methylmalonyl-CoA and the related acyclic acids methylmalonic acid, propionic acid, and 2-methyl citrate (1–4). This loss causes a lethal inborn error of metabolism known as methylmalonic acidemia (MMA), a common and severe organic acidemia (OA) (5).

Treatment options for patients with MMA are limited to dietary protein restriction, carnitine supplementation, clinical monitoring, and in severely affected children, elective liver/kidney transplantation (3, 6–13). Even with vigilant management, patients are prone to recurrent episodes of metabolic ketoacidosis and encephalopathy associated with hyperammonemia. Hyperglycinemia, reduced glutathione production, and more globally, a severe secondary mitochondriopathy affecting certain cell types such as hepatocytes characterize the disease in most patients. Multiple organ systems including the CNS, ocular, renal, hepatobiliary, cardiac, endocrine, and skeletal systems can manifest severe pathology with unclear causation. For example, the mechanism(s) predisposing patients to increased blood ammonia is undetermined. Similarly, MMA-associated dysfunction noted in other metabolic pathways including the urea cycle, the glycine cleavage system, the Krebs cycle, and ROS defense, have been widely attributed to toxic metabolites (14) without mechanistic validation.

That more than the circulating metabolic pool underlies the pathophysiology seen in MMA is supported by the clinical and biochemical phenotype of combined malonic and methylmalonic aciduria (CMAMMA). CMAMMA is most commonly caused by mutations in acyl-CoA synthetase family member 3 (ACSF3)(15–17), the enzyme responsible for converting free methylmalonic and malonic acid to methylmalonyl-CoA and malonyl-CoA in mitochondrial matrix (16, 17). CMAMMA, like MMA, is characterized by elevated concentrations of methylmalonic acid in body fluids, but without the accretion of the respective CoAs (16, 17). In stark contrast to patients with isolated MMA, patients with CMAMMA do not manifest intermediary metabolic disease symptoms. The disparate phenotypes presented by patients with different forms of MMA suggests that methylmalonyl-CoA rather than methylmalonic acid contributes to the manifestations of classical MMA.

Author Manuscript Author Manuscript Author Manuscript Author Manuscript

We hypothesized that aberrant acyl-CoA accretion in isolated MMA could perturb endogenous cellular homeostasis through the unregulated formation of CoA-derived covalent posttranslational modifications (PTMs)(18–22). Although the movement of acyl groups from acyl-CoA onto protein lysine residues is enzymatically driven by histone acetyltransferases (HATs) outside of the mitochondrial matrix(23–28), the alkaline conditions maintained in the mitochondrial matrix circumvent the need for enzymatic generation (18). Hence, in MMA and related OAs, an overabundance of mitochondrial acyl-CoA species generated as a consequence of the enzyme defect could create a unique environment for excessive, unregulated acylation (23, 27–31), with subsequent inhibition, and dysregulation, of diverse metabolic pathways(23, 29, 30). Here, we set out to examine the acylation landscape in liver explants from patients with MMA and various tissues from MMA mouse models compared to unaffected controls, and to establish methylmalonyl-lysine as a disease-specific PTM that impacts disease pathophysiology.

RESULTS

Hyperacylation characterizes the PTM landscape of MMA in humans and mice

We surveyed total acylation in tissue extracts from mouse models of methylmalonyl-CoA mutase deficiency and liver explants donated by patients with MMA. Hepatic extracts from $Mmut^{-/-};Tg^{INS\text{-}MCK\text{-}Mmut}$ mice, a model that recapitulates the hepatorenal mitochondriopathy of MMA (32), were studied using Western blot analysis with anti-malonyl, anti-succinyl, anti-acetyl, and anti-propionyl antibodies. We noted that the anti-malonyl antibody could also detect methylmalonylation, a form of acylation we identified with an in vitro assay (fig. S1). We noted grossly increased propionylation and malonyl/methylmalonylation in MMA mice compared to heterozygous control littermates, but did not see an observable change in succinylation or acetylation (FIG. 1A) (33, 34). Hepatic extracts from patients with MMA exhibited the same pronounced hyper-malonylation/methylmalonylation and propionylation compared to controls seen in the MMA mice (FIG. 1A–B) indicating these forms of hyper-acylation are specific to MMA and likely occur on conserved protein targets.

To further support the hypothesis that disease-related PTMs were dependent upon intramitochondrial malonyl- and methylmalonyl-CoA pools, we generated $Acsf3^{-/-}$ mice that recapitulate CMAMMA(35) and examined their liver extracts for PTMs. $Acsf3^{-/-}$ mice had reduced methylmalonylation and malonylation compared to $Mmut^{-/-};Tg^{INS\text{-}MCK\text{-}Mmut}$ mice and even less than littermate controls (FIG. 1C–D), indicating that accumulation of acylation PTMs seen in MMA derive from precursor CoA species (23, 27, 29, 30, 36–41) (42).

Tandem mass spectrometry profiling of the hepatic proteome in MMA mice reveals a landscape of aberrantly malonyl- and methylmalonylated proteins

To determine which metabolic pathways would be most adversely affected in MMA as a result of hyperacylation, we surveyed the hepatic proteome of MMA using LC-MS/MS. First, we generated anti-malonyl antibody immunoprecipitation columns and purified malonylated and methylmalonylated proteins from the hepatic extracts

Author Manuscript Author Manuscript Author Manuscript Author Manuscript

of *Mmut*$^{-/-}$;*Tg*$^{INS\text{-}MCK\text{-}Mmut}$ and control mice. Due to the cross-reactivity of the anti-malonyl-lysine antibody to methylmalonyl-lysine but not to succinyl-lysine and because succinylation was not elevated in MMA mice, we were able to enrich for proteins with malonylation or methylmalonylation PTMs. We distinguished the type of acylation on any given protein lysine residue prior to using tandem mass spectrometry as methylmalonylation and succinylation are isobaric. We then subjected the resulting proteins to gene ontology analysis (43, 44). Enrichment of malonylation and methylmalonylation PTMs on multiple enzymes that function in metabolic pathways such as glutathione production, the urea cycle, arginine biosynthesis, and oxidoreduction were present in MMA samples versus controls, and modeled using KEGG ontology into protein network webs via NetworkAnalyst (45–49) (FIG. 2A–B). Many of the hits mapped into pathways critical to mitochondrial and intermediary metabolism, further suggesting that hyperacylation resulting from increased disease specific acyl-CoA pools could have pathophysiological consequences.

We also observed increased acylation of multiple urea cycle enzymes including CPS1, Arginase 1 (ARG1), argininosuccinate lyase (ASL), and argininosuccinate synthase (ASS1) in MMA mice. CPS1 exhibits increased malonylation or methylmalonylation on 15 different lysine residues in MMA mice compared to controls, including sites previously established to be associated with CPS1 inactivation (lysine 1291) and impaired ureagenesis (50). To validate these modifications of CPS1, we repeated the purification of malonylated/methylmalonylated proteins from hepatic tissue extracts of *Mmut*$^{-/-}$;*Tg*$^{INS\text{-}MCK\text{-}Mmut}$ and control mice. We noted increased capture of malonylated/methylmalonylated CPS1 from MMA mouse tissue samples compared to controls despite lower total CPS1 abundance in MMA mice (FIG. 2C).

We then examined CPS1 enzymatic activity in vitro using a well-established assay previously used in the clinical diagnosis of CPS1 deficiency (51). CPS1 enzymatic activity from hepatic tissue extracts was lower in *Mmut*$^{-/-}$;*Tg*$^{INS\text{-}MCK\text{-}Mmut}$ mice compared to controls (**p<0.01, **p=0.0026) (FIG. 2D), further indicating malonylation and methylmalonylation negatively impact CPS1 activity in MMA. We also performed immunoprecipitation analysis on CPS1 directly from human hepatic MMA tissue samples and control samples: patients had malonylation/methylmalonylation of CPS1 but there was no detectable malonylation/methylmalonylation in unaffected donors (FIG. 2E). Therefore, disease specific hyper-malonylation/methylmalonylation of CPS1, and potentially other urea cycle enzymes, could account for the impairment of the proximal urea cycle and subsequent propensity toward hyperammonemia that is common in MMA.

A number of Krebs cycle proteins including malate dehydrogenase 2 (MDH2), citrate synthase (CS), isocitrate dehydrogenase (IDH2), dihydrolipoyllysine-residue succinyltransferase (DLST), and aconitase 2 (ACO2) were also aberrantly modified in MMA mice. These enzymes, along with 2-oxoglutarate dehydrogenase (OGDH), had increased abundance of immunoreactive enzymes (FIG 2F) and increased global malonyl/methylmalonylation (FIG 2G) in hepatic extracts from *Mmut*$^{-/-}$;*Tg*$^{INS\text{-}MCK\text{-}Mmut}$ mice compared to controls. Glutamate dehydrogenase 1 (GDH1), which has previously been identified as a possible target of pathology in MMA (52), exhibited both methylmalonylation and malonylation, specifically at K503 (Fig. S2A). We confirmed increased malonyl or

Author Manuscript Author Manuscript Author Manuscript Author Manuscript

methylmalonylation of GDH1 when purified from MMA murine liver tissue samples compared to control samples (FIG. 2H). Acetylation of K503 may increase enzymatic activity due to the location of this residue in the GTP binding pocket of GDH1 (53). Thus, for this target, increased malonyl or methylmalonylation of K503 could lead to increased enzymatic activity and paradoxically activate glucose metabolism, which is dysregulated in MMA (54). Overall, the proteomic data from MMA mice revealed that aberrant acylation was present on numerous proteins in pathways that display impaired activity in the disease state, and for selected hits, was confirmed in human liver samples.

Effects of aberrant acylation on mitochondrial DNA maintenance

To explore the basis of the electron transport chain (ETC) dysfunction in tissues affected by MMA mitochondriopathy, we performed targeted exploration of low abundance proteins, such as those involved in mitochondrial DNA maintenance, that might not have been detected by mass spectrometry. We first examined mitochondrial transcription factor A (TFAM), which localizes to the mitochondria where it stabilizes mtDNA, maintains mtDNA copy number, and regulates the expression of mtDNA genes such as electron transport chain subunits (55). Total TFAM protein abundance was not reduced in MMA mouse hepatic or renal tissues compared to controls (FIG. 3A–B), indicating loss of mtDNA expression is not the result of reduced TFAM. Increased malonylation/methylmalonylation of TFAM was evident in hepatic and renal tissues of MMA mice but not controls (FIG. 3A–B). Initial tandem mass spectrometry analysis indicated POLRMT, an essential mtDNA transcription enzyme recruited to mtDNA promoters by TFAM to form a transcription complex with mitochondrial transcription factor B2 (TFB2m) (56), exhibited increased malonylation in MMA hepatic extracts compared to controls. We confirmed increased malonylation via co-immunoprecipitation with TFAM, and additionally discovered POLRMT exhibits increased propionylation in MMA mice compared to controls (FIG. 3A). Increased acylation of these transcription factors, especially with negatively charged PTMs such as malonylation and methylmalonylation, could lead to diminished activity (55) and subsequently reduced mtDNA copy number and reduced transcription of mtDNA-encoded ETC subunits. To explore whether DNA depletion might be present in hepatocytes, a cell that that typically displays the secondary enzymatic and mitochondrial manifestations seen in MMA, we examined mtDNA copy number in both human and mouse MMA liver extracts compared to controls. We found that both human (*$p<0.05$, $p=0.0221$ ND6, $p=0.0246$ COXI) and mouse MMA tissue (****$p<0.0001$, $p=0.00003$ ND6) exhibited significantly reduced mtDNA copy number compared to their respective controls (FIG. 3C–D), identifying a putative mechanism to explain the ETC defect that classically accompanies MMA (32, 57–59).

Methylmalonylation of components of the glycine cleavage system explains MMA-associated hyperglycinemia

Patients with methylmalonic acidemia, propionic acidemia, and isovaleric acidemia classically display hyperglycinemia, which were historically considered forms of ketotic hyperglycinemia (KH) (60–63). However, despite the fact that organic acidemias have been recognized as a cause of KH since the 1960s, the causative molecular mechanism for increased glycine has yet to be uncovered (60–63). To probe the underlying mechanism of hyperglycinemia in MMA, we began by examining enzymes of the

Author Manuscript Author Manuscript Author Manuscript Author Manuscript

glycine cleavage system in hepatic tissue samples from patients with MMA compared to unaffected donors. MMA livers exhibited a consistent decrease in glycine dehydrogenase (GLDC) compared to controls but had increased aminomethyltransferase (GCST/AMT), dihydrolipoyl dehydrogenase (DLD), and glycine cleavage H protein (GCSH) (FIG. 4A). This increase in DLD, GCST, and GCSH could potentially be attributable to increased mitochondrial mass seen in MMA via megamitochondria formation (32, 57).

Because acylation PTMs occupy lysine residues, we explored whether aberrant acylation could effectively block the placement of lipoic acid by lipoyltransferase 2 (LIPT2) and lipoyl synthase (LIAS) on GCSH. Overall, liver tissues from patients with MMA exhibited increased lipoylation PTMs compared to controls, likely due to increased mitochondrial mass, with the exception of one band at 15–18 kDa that exhibited lipoylation in control but not MMA samples (FIG. 4B). We suspected this band was GCSH, the only protein at this molecular weight that is known to be lipoylated. We performed an immunoprecipitation analysis against GCSH (or IgG control) from hepatic tissue samples from patients with MMA and stained for lipoylation and total GCSH protein. We confirmed that GCSH was lipoylated in unaffected donor tissues but not in MMA liver extracts (FIG. 4C). To determine if aberrant acylation of GCSH was present, we generated an antibody that specifically recognized methylmalonylation (Fig. S3) and performed immunoprecipitation against GCSH or IgG control. We observed increased methylmalonylation of GCSH from MMA samples but not controls (FIG. 4D). These results suggest that methylmalonylation of GCSH on or near catalytic lysine residueK107 inhibits placement of lipoic acid by LIPT2/LIAS (64). Without lipoylation, GCSH would not be able to shuttle the methylamine group from GLDC for degradation by GCST. The lack of lipoylation combined with reduced abundance of GLDC likely explains the association of MMA with hyperglycinemia.

In parallel, we confirmed the pattern of decreased GLDC expression, loss of lipoylation of GCSH, and aberrant methylmalonylation of GCSH in MMA mouse liver tissues compared to heterozygous controls, finding these modifications are conserved (FIG. 4E). Additionally, GCSH abundance and modification were normal in MMA mice that harbored a liver-specific transgene ($Mmut^{-/-};Tg^{INS\text{-}Alb\text{-}Mmut}$) (FIG. 4F), further supporting the hypothesis that loss of MMUT function and subsequent disease pathophysiology is driven by methylmalonyl-CoA derived PTMs.

Loss of function of Sirt5 increases disease severity in MMA mice

Because sirtuin (SIRT) enzymes are essential in maintaining metabolic homeostasis through the removal of acylation PTMs (65–67), we surveyed SIRTs using a modified in vitro assay we developed where purified BSA is specifically modified with various acyl groups and then used as a substrate to probe deacylase activity and substrate preference. SIRT5 and SIRT1 exhibited the strongest activity against methylmalonylation and propionylation in vitro (fig. S5). Because SIRT5 is mitochondrially localized and has a preference for negatively charged acylation modifications including malonylation (27), we posited that a loss of SIRT5 activity would likely result in increased disease severity in MMA due to an escalation of methylmalonylation. Using a genetic approach, we generated a double mutant line mouse line, $Sirt5^{-/-};Mmut^{G715V/G715V}$, by breeding mice with a partial deficiency form

Author Manuscript Author Manuscript Author Manuscript Author Manuscript

of isolated MMA (*Mmut*$^{G715V/G715V}$) (68) with those carrying a *Sirt5* loss of function allele (69).

As predicted, *Sirt5*$^{-/-}$;*Mmut*$^{G715V/G715V}$ mice were more severely affected with MMA and significantly runted (*$p<0.05$, *$p=0.03$ *at 2.75 months*, **$p<0.01$, **$p=0.0048$ at 4 months, **$p=0.0028$ at 5 months, and **$p=0.0032$ at 6 months) compared to *Sirt5*$^{+/-}$;*Mmut*$^{G715V/G715V}$ littermates (FIG. 5A). Hepatic protein extracts were analyzed for global methylmalonylation and propionylation PTMs, as well as β-actin and SIRT5 expression. Mice with *Mmut*$^{G715V/G715V}$ genotypes exhibited the highest amount of methylmalonylation marks when they also lacked both *Sirt5* alleles, followed by *Sirt5*$^{+/-}$;*Mmut*$^{G715V/G715V}$ and *Sirt5*$^{+/+}$;*Mmut*$^{G715V/G715V}$ mice (FIG. 5B). These results further indicated that SIRT5 recognizes and removes excessive methylmalonylation PTMs in vivo. However, propionylation marks remained consistent between these genotypes indicating that SIRT5 preferentially removes negatively charged PTMs over neutral charged PTMs in vivo (FIG. 5C). Last, a functional effect on ureagenesis was assessed by measuring ammonia concentrations in plasma from terminal bleeds, with *Sirt5*$^{-/-}$;*Mmut*$^{G715V/G715V}$ mice exhibiting elevated blood ammonia compared to control genotypes (***p<0.001, $p=0.0002$) (FIG. 5D). In aggregate, the data presented here demonstrate an explanation for disease pathophysiology in MMA and provide proof of concept for the exploration of an adjunct deacylase therapy as a treatment for MMA.

Engineering an acylation inhibition-resistant SIRT5 for therapeutic application in MMA

Because SIRT5 would be essential to the reduction of methylmalonylation in MMA, we examined endogenous abundance of SIRT5 in MMA mouse (*Mmut*$^{-/-}$;*Tg*$^{INS\text{-}MCK\text{-}Mmut}$) and patient liver tissue samples. Using Western blot analysis, we found SIRT5 protein abundances were uniformly reduced in MMA hepatic protein extracts compared to respective controls (FIG. 6A–B). We also determined that SIRT4, SIRT7, and SIRT6 abundances were reduced whereas SIRT1 and SIRT3 were elevated in MMA mice (FIG 6A) whereas patients with MMA exhibited reductions in SIRT4, SIRT3, and SIRT1 compared to unaffected donors (FIG 6B). We previously determined if differences in Sirtuin protein abundance in *Mmut*$^{-/-}$;*Tg*$^{INS\text{-}MCK\text{-}Mmut}$ mice could be a change in gene expression by examining a transcriptomic microarray data set produced for this mouse line, and found no significant difference in any of the Sirtuin mRNA abundances between MMA mice and controls (32). Therefore, differences in SIRT abundances may be post-transcriptionally mediated, by translation, protein stability, or turnover. Although changes in the abundances of various Sirtuins were variable, the consistent depression of SIRT5 may potentiate the disease phenotype, given we established its activity as a demethylmalonylase. To test the potential therapeutic benefit of increasing SIRT5 activity as a treatment for MMA, we delivered SIRT5 to *Mmut*$^{-/-}$;*Tg*$^{INS\text{-}MCK\text{-}Mmut}$ and *Mmut*$^{+/-}$;*Tg*$^{INS\text{-}MCK\text{-}Mmut}$ mice using systemic AAV gene therapy. Because *in vitro* studies indicated that SIRT5, when acylated, led to decreased enzymatic activity (fig. S5A), we first engineered a modified version of the SIRT5 enzyme, designated SuperSIRT5, using conservation analysis and site-directed mutagenesis. SuperSIRT5 retained enzymatic activity under hyperacylation conditions and also exhibited resistance to inhibition by nicotinamide *in vitro* (fig. S6B–C).

Author Manuscript Author Manuscript Author Manuscript Author Manuscript

Using a retro orbital delivery route, we then treated *Mmut*$^{-/-}$;*Tg*$^{INS\text{-}MCK\text{-}Mmut}$ and *Mmut*$^{+/-}$;*Tg*$^{INS\text{-}MCK\text{-}Mmut}$ mice between 2 and 3 months of age with a liver-specific SuperSIRT5-FLAG AAV8 vector or similar GFP control and monitored the mice over 8 months. 4 of the 6 SuperSIRT5 treated *Mmut*$^{-/-}$;*Tg*$^{INS\text{-}MCK\text{-}Mmut}$ mice exhibited high levels of SuperSIRT5-Flag expression as assessed by Western blot analysis of liver tissue extracts (fig. S4C). These four mice demonstrated a significant increase in percent body weight compared to GFP-treated *Mmut*$^{-/-}$;*Tg*$^{INS\text{-}MCK\text{-}Mmut}$ control mice (*p<0.05, *p=0.039 at 3 months, *p=0.017 at 3 months, and *p=0.039 at 3 months)) indicating SIRT5 activity mitigated the disease phenotype, presumably via reversal of excessive MMA-specific PTMs (FIG. 6C). Indeed, *Mmut*$^{-/-}$;*Tg*$^{INS\text{-}MCK\text{-}Mmut}$ mice that expressed SuperSIRT5-FLAG exhibited reduced global methylmalonylation compared to GFP-treated *Mmut*$^{-/-}$;*Tg*$^{INS\text{-}MCK\text{-}Mmut}$ controls, supporting the in vivo efficacy of SuperSIRT5 as a demethylmalonylase (FIG. 6C–D).

Further analysis of a candidate target, CPS1, in hepatic extracts from SuperSIRT5 and GFP-treated control mice (FIG. 6E) demonstrated that SuperSIRT5 treatment led to reduced methylmalonylation. Functionally, SuperSIRT5-treated *Mmut*$^{-/-}$;*Tg*$^{INS\text{-}MCK\text{-}Mmut}$ mice, as compared to GFP-treated *Mmut*$^{-/-}$;*Tg*$^{INS\text{-}MCK\text{-}Mmut}$ and untreated *Mmut*$^{-/-}$;*Tg*$^{INS\text{-}MCK\text{-}Mmut}$ mice, demonstrated decreases in blood ammonia concentrations (FIG. 6F). SuperSIRT5-treated *Mmut*$^{-/-}$;*Tg*$^{INS\text{-}MCK\text{-}Mmut}$ mice also exhibited restored lipoylation of GCSH (FIG. 6G), further demonstrating how a Sirtuin-based therapy could mitigate MMA pathophysiology. We also examined endogenous protein abundances of the other urea cycle enzymes in both *Mmut*$^{-/-}$;*Tg*$^{INS\text{-}MCK\text{-}Mmut}$ and *Mmut*$^{-/-}$;*Tg*$^{INS\text{-}MCK\text{-}Mmut}$ mice treated with SuperSIRT5-FLAG AAV8 or GFP AAV8 (FIG S6B). Doing so allowed us to further demonstrate decreased ammonia concentrations in SuperSIRT5-FLAG-treated MMA mice was likely the result of decreased PTMs on CPS1 and not due to altered abundances of urea cycle enzymes. Western blot analysis revealed that the total abundance of each urea cycle enzyme, CPS1, ASL, ASS1, OTC, and ARG1 was not altered between treatment groups (fig. 3 SB). In fact, both CPS1 and OTC had increased protein abundances in MMA mouse liver tissues, likely as a result of increased mitochondrial mass (fig. S4 B) (32).

DISCUSSION

The organic acidemias, as a group of metabolic disorders, are among the most common inborn errors of metabolism (70). However, despite efforts to identify affected individuals early in life by newborn screening, many patients, especially those with MMA and related disorders, continue to experience disease symptoms despite aggressive dietary and medical management. Although previous theories have focused on the toxicity of acylic acids as the primary cause of disease pathophysiology (4), the accretion of circulating toxic metabolites alone cannot account for the wide array of OA symptoms and secondary metabolic perturbations.

Here we have discovered a disease mechanism likely common to all OAs and potentially other forms of metabolic disease: the accumulation of aberrant acylation PTMs on enzymes in critical intracellular pathways. A wide array of proteins exhibited substantially

Author Manuscript Author Manuscript Author Manuscript Author Manuscript

altered acylation in hepatic protein extracts from human patients with MMA and well as hepatic, neuronal, and renal protein lysates from MMA murine models. The pattern of PTM accumulation was highly conserved between species, indicating modification occurs consistently on specific proteins and further providing evidence that this unbalanced PTM axis contributes to the disease phenotypes.

Mass spectrometry analysis confirmed that aberrant acylation was heavily enriched on mitochondrial, metabolic regulatory proteins including those in key cellular pathways known to be dysregulated in MMA. We found that CPS1, Krebs cycle enzymes, and GDH1 in MMA mice were marked with increased acylation PTMs. In the cases of CPS1 in the urea cycle and the enzymes of the Krebs cycle, aberrant acylation is predicted to decrease enzymatic activity. In the case of GDH1, methylmalonylation and malonylation of K503 could increase enzymatic activity due to its location in the allosteric binding site for the GDH1 inhibitor GTP (53) Specifically, by reversing the positive charge on lysine to negative, malonylation or methylmalonylation would diminish binding of GTP, thus increasing GDH1 activity (53) and subsequently dysregulating glucose metabolism.

An analysis of candidate targets not detected by mass spectrometry methods revealed hyperacylation and potential disruption of mitochondrial DNA regulatory transcription factors. We also found evidence of acylation driven disruption of the GCS providing mechanistic insights into the basis of MMA associated mitochondriopathy and the reason underlying a mysterious and prominent secondary metabolic perturbation seen in several OAs. Through these studies we not only identified a new disease mechanism in MMA but also discovered a disease-specific form of PTM that we termed methylmalonylation. Although propionylation and malonylation PTMs are well known, we suspected that methylmalonyl acyl groups could be also recruited as lysine PTMs, especially in the mitochondrial environment in MMA where there are high concentrations of methylmalonyl-CoA in the matrix. After we confirmed that methylmalonylation could occur non-enzymatically in vitro, and we generated an antibody against methylmalonylated lysine that demonstrated weak cross-reactivity to malonylated lysine but had no cross reactivity to propionylated or succinylated lysine. We then demonstrated reactivity of the purified antibody only to methylmalonylation in vitro and through Western blotting of hepatic tissue samples from patients with MMA compared to unaffected donors. Hepatic, brain, and renal tissues from MMA mice further demonstrated that methylmalonylation is a disease-specific modification and is present in target tissues where pathology develops. This reagent should be useful for the development of biomarker assays for monitoring disease progression and assess the efficiency of new treatments that target the aberrant acylome of MMA.

The discovery of methylmalonylation presented a subsequent challenge to discern whether a mechanism(s) was present to reverse its placement, especially since methylmalonylation was not detectable in controls. Acylation PTMs, especially those in the mitochondria, are normally metabolized by the deacylase enzyme family known as the Sirtuins (67). Of the 7 SIRTs, SIRT1 and SIRT5 exhibited the strongest demethylmalonylase activity. Although we observed variation in other Sirtuins, which differed across species, SIRT5 was pursued as the lead deacylase because it localizes to the mitochondria, has an established preference for negatively charged acylation PTMs (50), and we established that it functions as a

Author Manuscript Author Manuscript Author Manuscript Author Manuscript

demethylmalonylase in vitro. We then explored the effects of loss of function of *Sirt5* in a genetic study. Using a partial deficiency MMA mouse model (*Mmut*$^{G715V/G715V}$), the loss of function of *Sirt5* worsened the MMA-related phenotypes. Therefore, although not directly involved in the catabolism of methylmalonyl-CoA, SIRT5 is essential to the regulation of aberrant acylation marks in MMA, and likely other OAs where negatively charged acylation marks may accumulate.

Insights from in vitro biochemical studies taken together with the accentuated disease phenotype displayed by *Sirt5*$^{-/-}$;*Mmut*$^{G715V/G715V}$ mice provided strong proof of concept for the development of a SIRT5 therapeutic for MMA. Because endogenous SIRT5 protein abundance was uniformly diminished in mice and patients with MMA, with further enzymatic activity greatly reduced by propionylation or methylmalonylation, we engineered a SIRT5 enzyme, termed SuperSIRT5, that maintained activity even when aberrantly acylated or in the presence of the natural sirtuin inhibitor nicotinamide. We used an AAV8 vector configured to express SuperSIRT5 under the control of a liver-specific promoter and delivered the virus to *Mmut*$^{-/-}$;*Tg*$^{INS\text{-}MCK\text{-}Mmut}$ mice. SuperSIRT5 expression lowered inhibitory methylmalonylation on key enzymes such as CPS1 and resulted in increased weight gain, lowered blood ammonia concentrations, re-establishment of lipoylation on GCSH in MMA mice. Although we noted an improved phenotype in the treated *Mmut*$^{-/-}$;*Tg*$^{INS\text{-}MCK\text{-}Mmut}$ mice, hepatic expression of SuperSIRT5 did not decrease blood methylmalonic acid concentrations, further demonstrating that aberrant acylation likely contributes more significantly to secondary enzymatic dysfunction as compared to the accumulation of the corresponding acylic acid. Although the disease mechanisms of organic acidemias are multifaceted, our studies have led to the proposal of a PTM centric model to interpret the complex pathophysiology of MMA.

Herein, we established a mechanism for disease pathophysiology in OAs broadly extendable to genetic and environmental causes of deranged vitamin B12 metabolism (fig. S7) and developed a treatment approach that might be applied to disorders where intramitochondrial coenzyme A accretion is pathogenic. Current gene or mRNA therapies therapies aimed at partially restoring MMUT, via gene or mRNA therapies, could be diminished by aberrant acylation in the disease mileau. Therefore, conventional genomic therapies might benefit from a small molecule adjunct deacylase therapy, and in OAs without any treatments in place, deacylase activators, and perhaps AAV gene therapy with SuperSIRT5, could potentially serve as a therapeutic.

Through combined mouse and human studies, we identified a candidate regulatory axis that includes SIRT5 as a critical deacylase in MMA but there are several limitations that warrant further discussion. We documented that other SIRTs, such as 1, 3, and 4, were reduced. These sirtuins catalyze deacylation reactions, some with substrate overlap with SIRT5. Moreover, the decrease in SIRT1 has been observed in other disorders of vitamin B12 metabolism (71). The roles of the other SIRTs as mediators of pathophysiology remain unclear as we were unable to explore the matter further herein. We are also limited in that we did not examine off-target effects of overexpression of SIRT5 as a potential therapy. Furthermore, we noted that the enzymes of the urea cycle were intact, although the activities of each may be subject to additional regulation that has yet to be explored via additional

Author Manuscript Author Manuscript Author Manuscript Author Manuscript

proteomic analyses and examination of epigenetic effects (72). The spectrum of effects mediated by PTMs is growing (73), and our studies firmly establish a critical role for SIRT5 in mediating the biochemical perturbations observed in MMA, and, we believe, related disorders.

MATERIALS AND METHODS

Study design

The aim of this study was to demonstrate the impact of aberrant acylation of metabolic enzymes on MMA pathogenesis and to examine the therapeutic benefit of a deacylase-directed therapy. We first analyzed the acylation landscape of murine MMA and control liver tissues by Western blot, immunoprecipitation, and mass spectrometry analysis. We validated mass spectrometry results on multiple key metabolic enzymes purified from murine and human MMA liver tissue and respective controls (minimum n=3 for each group) via Western blot and immunoprecipitation analysis. We also examined aberrant acylation on low abundance enzymes not detected by mass spectrometry using Western blot and immunoprecipitation analyses (n=3 per group). In some instances, enzymatic function was assessed via in vitro enzymatic assay (n=3 per group) or using RT-PCR (n=3 per group) to measure relative expression.

We next examined the therapeutic potential of deacylase enzymes. We determined SIRT5 to be the most effective demethylmalonylase using an in vitro assay. To establish an in vivo role for acylation, we examined the effect of SIRT5 loss of function in a partial deficiency MMA mouse model. Mice with *Sirt5* and *Mmut* mutations were examined for acylation abundance (n=1 to n=4), body weight (n=6 to n=19), and blood ammonia concentrations (n=1 to n=11). To protect SIRT5 from inactivation in the setting of MMA, we used conservation analysis and site-directed mutagenesis to generate an acylation-resistant SuperSIRT5-FLAG enzyme and used in vitro assays to confirm activity was intact.

To examine the therapeutic benefit of SuperSIRT5 in MMA, we packaged SuperSIRT5-FLAG in an AAV8 under a liver specific promoter and used this vector to treat 6 $Mmut^{-/-};Tg^{INS\text{-}MCK\text{-}Mmut}$ mice and 3 $Mmut^{+/-};Tg^{INS\text{-}MCK\text{-}Mmut}$ mice. A similarly configured GFP control vector was injected into 5 $Mmut^{-/-};Tg^{INS\text{-}MCK\text{-}Mmut}$ mice and 3 $Mmut^{+/-};Tg^{INS\text{-}MCK\text{-}Mmut}$ mice. One GFP treated and 3 $Mmut^{-/-};Tg^{INS\text{-}MCK\text{-}Mmut}$ mice died early in the study reducing n to 4 and only 4 SuperSIRT5-FLAG treated $Mmut^{-/-};Tg^{INS\text{-}MCK\text{-}Mmut}$ mice exhibited SuperSIRT5-FLAG expression via Western blot analysis and were included in weight data records (n=4 for each $Mmut^{-/-};Tg^{INS\text{-}MCK\text{-}Mmut}$ group and n=3 for each $Mmut^{+/-};Tg^{INS\text{-}MCK\text{-}Mmut}$ group). Ammonia was measured in blood from the same mice as well as 3 untreated $Mmut^{-/-};Tg^{INS\text{-}MCK\text{-}Mmut}$ mice and 3 untreated $Mmut^{+/-};Tg^{INS\text{-}MCK\text{-}Mmut}$ mice. Power analysis/calculations were not used in this study to select sample sizes; samples were not randomized, and experimenters were not blinded. Mouse experiments were carried out over a course of 6–12 months due to COVID-related personnel restrictions.

Author Manuscript Author Manuscript Author Manuscript Author Manuscript

SuperSIRT5 mutagenesis

Using conservation analysis and site directed mutagenesis, we made a modified version of SIRT5-FLAG (Addgene plasmid #13816) we renamed to SuperSIRT5-FLAG. We performed conservational analysis of the 9 lysines within the deacylase domain of human SIRT5 protein sequence (amino acids 58–255) using Protein Blast (74) to compare the human sequence (NP_001363727.1) to the SIRT5 sequences found in chimpanzee (XP_001169506.2), mouse (NP_849179.1), frog (NP_001263631.1), chicken (NP_001263293.1), zebrafish (6FKY_A), and fruit fly (NP_572241.2). Sites with low conservation or lack of conservation in human, chimpanzee, and mouse were eliminated as potential targets. Lysines that were documented to by ubiquitinated by PhosphoSitePlus (75) were eliminated as targets as they were likely involved in proper protein turnover. The remaining 5 residues were run through PolyPhen-2 (76) to determine if mutation from lysine to arginine would be benign to protein function through more in depth conservation analysis. We then examined the crystal protein structure of SIRT5 (Research Collaboratory for Structural Bioinformatics Protein Data Bank or RCSB PDB, structure 5XHS) (77) and determined to modify 4 of these 5 lysines based on their proximities to the deacylase catalytic and co-factor binding pockets. Lysines modified to arginine included K79, K112, K148, and K152. This SIRT5 was resistant to acylation-based inhibition of enzymatic function and also demonstrated reduced inhibition by nicotinamide.

Mouse Models

Animal work was performed in accordance with the guidelines for animal care at NIH and the Guide for the Care and Use of Laboratory Animals. For the $Acsf3^{-/-}$ mouse line, a C57BL/6J BAC clone containing the murine *Acsf3* gene was used to prepare a targeting construct. Through homologous recombination, the first coding exon of the murine *Acsf3* gene (exon 2) was replaced with a neomycin resistance marker cassette in B6.129 embryonic stem cells. Briefly, we cloned the 5’ end of the gene in a pPNT vector containing a neomycin resistance gene flanked by locus of X(cross)-over in P1 (loxP) sites. These loxp sites in turn were flanked by a 5’ homology arm to *Acsf3* exon 1 upstream and a 3’ homology arm to *Acsf3* exons 3 and 4 downstream. The 3’ arm was cloned in pPNT non-specifically with EcoRI found on the vector and tested for orientation. We also incorporated the Herpes Simplex Virus-1 Thymidine Kinase (HSV-TK) gene downstream of the 3’ homology arm. Cloning of the 5’ homologous arm required linearizing the construct via incorporated Not1 and Ssp1 restriction sites in. ES clones were screened using combination of long-range PCR/enzyme digestion and Southern blotting. Primers that flank the 5’ loxP were used to genotype the animals. The resulting murine embryonic stem cells were microinjected into murine blastocysts and then implanted into female mice mated with a vasectomized male. The resulting chimeras were screened for germline $Acsf3^{-/+}$ transmission and positive founders were used in further breeding to generate the knockout mouse line.

For the $Mmut^{-/-};Tg^{INS\text{-}MCK\text{-}Mmut}$ and $Mmut^{-/-};Tg^{INS\text{-}Alb\text{-}Mmut}$ mouse lines, see the methods as previously described in (32) (58). For the $Sirt5^{-/-};Mmut^{G715V/G715V}$ mouse line, B6;129-$Sirt5^{tm1Fwa/J}$ mice from the Jackson Laboratory (JAX stock #012757) (69) were crossed to the $Mmut^{G715V/G715V}$ (68) line to generate mice heterozygous for both

Author Manuscript Author Manuscript Author Manuscript Author Manuscript

mutant alleles. Heterozygous mice were then crossed to generate *Sirt5*$^{+/-}$; *Mmut*$^{+/G715V}$ and *Sirt5*$^{-/-}$; *Mmut*$^{+/G715V}$ females and *Sirt5*$^{-/-}$; *Mmut*$^{G715V/G715V}$ males, which were then crossed to the *Sirt5*$^{-/-}$; *Mmut*$^{+/G715V}$ females to generate double mutant *Sirt5*$^{-/-}$; *Mmut*$^{G715V/G715V}$ mice. Weights were recorded every week following weaning at 3 weeks of age. At 6 months of age, mice were euthanized following retro-orbital bleeding and organs were harvested and snap frozen before storage at −80°C.

Patient and control human liver samples

Patient studies were approved by the National Human Genome Research Institute Institutional Review Board as part of the NIH study "Clinical and Basic Investigations of Methylmalonic Acidemia and Related Disorders" (Clinicaltrials.gov, NCT00078078) and performed in compliance with the Declaration of Helsinki. Patients or their parents/legal guardians provided informed consent. Three MMA patient liver tissues were used consistently throughout this manuscript with genotypes: *MMUT* c.671_678dup, p.Val227fs/c.1022dup, p.Asn341fs; *MMUT* c.349G>T, p.Glu117Ter/ c.1038_1040del, p.Leu347del; and *MMUT* c.2053_2055dup, p.Leu685dup/c.2053_2055dup, p.Leu685dup. These were snap-frozen specimens from explanted native livers removed during an orthotopic liver transplantation procedure. Unaffected donor liver samples were obtained from adults who had undergone liver resection, usually after trauma, and then donated their liver tissues to the University of Pittsburgh cell isolation facility (Pittsburgh, PA, USA), established as part of an NIH-funded liver tissue cell distribution system. The collection of resected liver specimens was approved by the University of Pittsburgh Institutional Review Board (IRB Number 0411142) (54).

SuperSIRT5 AAV gene therapy

Six *Mmut*$^{-/-}$;*Tg*$^{INS\text{-}MCK\text{-}Mmut}$ and three *Mmut*$^{+/-}$;*Tg*$^{INS\text{-}MCK\text{-}Mmut}$ mice were treated with 1×10^{13} GC/kg of an AAV8 vector (retro-orbital injection) that encapsulated a transgene that uses the thyroxine binding globulin (TBG) promoter to drive the expression of SuperSIRT5-FLAG in the liver, abbreviated AAV8 TBG SuperSIRT5. Five *Mmut*$^{-/-}$;*Tg*$^{INS\text{-}MCK\text{-}Mmut}$ and three *Mmut*$^{+/-}$;*Tg*$^{INS\text{-}MCK\text{-}Mmut}$ were treated with 1×10^{13} GC/kg of an AAV8 TBG SuperSIRT5-FLAG or a AAV8 TBG GFP control. Mice were between 2 and 3 months of age and were weighed before treatment and then twice a week every week following treatment. At 8 months of age, mice were euthanized following retro-orbital bleed and organs were harvested and snap frozen before storage at −80°C.

Statistical analysis

In mass spectrometry analysis a 1% FDR was used for peptides (including PTM peptides) and proteins. For the following experiments all data sets were assessed for normality and logonomality in GraphPad/PRISM 8 via the Anderson-Daring test, D'Agnostino8 & Person test, Shaprio-Wilk test and Kolmogorov-Smirnov test. For all data sets, most normality assessments were incompatible because the sample size was too small. In cases where the normality was assessable, alpha=0.05). For CPS1 activity, measurements of activity from spectrophotometer were normalized to relative CPS1 protein abundance in MMA vs control murine live tissues (CPS1 abundances were on average 1.3x higher in MMA due to increased mitochondrial mass as measured in Image Studio). Significance was

Author Manuscript Author Manuscript Author Manuscript Author Manuscript

determined using an unpaired Welch's corrected t-test GraphPad Prism 8. For mtDNA copy number measurements, ND6 and/or COX1 were normalized to measurements of a control nuclear gene (β-actin). Significance was determined using an unpaired Welch's corrected t-test. Results were deemed significant at a $p<0.05$. For body weight measurements in the $Sirt5^{-/-};Mmut^{G715V/G715V}$ study, multiple t-tests were performed with Holm-Sidak correction method. Each row was analyzed individually, without assuming a consistent standard deviation in GraphPad.Prism 8. Results were deemed significant at a $p<0.05$. For ammonia assay measurements in the $Sirt5^{-/-};Mmut^{G715V/G715V}$ study, Welch's corrected T-tests were performed in GraphPad. Prism 8. Results were deemed significant at a $p<0.05$. For body weight measurements in the SuperSIRT-FLAG study, multiple t-tests with Holm-Sidak correction method were performed for each time point. Each row was analyzed individually, without assuming a consistent standard deviation in in GraphPad.Prism 8. Results were deemed significant at a $p<0.05$. For ammonia assay measurements in the SuperSIRT-FLAG study, an unpaired Welch's corrected t-test was performed in GraphPad Prism 8. Results were deemed significant at a $p<0.05$.

Supplementary Material

Refer to Web version on PubMed Central for supplementary material.

Funding:

PEH was supported by a Postdoctoral Research Associate (PRAT) fellowship from the National Institute of General Medical Sciences (NIGMS), award number 1FI2GM137781-01. YC and MG were supported by the were supported by the Intramural Research Program of the NHLBI. SM, JLS, CW, ND, PH, DC, AG, IM, and CPV were supported by the Intramural Research Program of the NHGRI through 1ZIAHG200318-16.

PEH and CPV are co-inventors on a provisional patent (Aberrant Post-Translational Modifications (PTMs) in Methyl-And Propionic Acidemia and a Mutant Sirtuin (SIRT) to Metabolize PTMs, Patent Application No. PCT/US2021/028228, Publication No. WO2021/225781) based on discoveries related to this work and filed on their behalf by the NIH.

Data and Materials Availability:

All data associated with this study are in the paper or the Supplementary Materials. Reagents and materials associated with this study are available from the corresponding author (C.V.) after completion of an MTA. Malonylated and methylmalonylated peptides from mass spectrometry on MMA mice are given in data files S1 and S2, respectively.

References

1. Fenton WA, Gravel RA, and Rosenblatt DS, in The Metabolic and Molecular Bases of Inherited Disease, Scriver ALBCR, Sly WS, and Valle D, eds., Ed. (McGraw-Hill, New York, 2001), pp. 2165–2193.
2. Manoli I, Sloan JL, Venditti CP, in GeneReviews((R)), Adam MP, Ardinger HH, Pagon RA, Wallace SE, Bean LJH, Stephens K, Amemiya A, Eds. (Seattle (WA), 1993).
3. Fraser JL, Venditti CP, Methylmalonic and propionic acidemias: clinical management update. Curr Opin Pediatr 28, 682–693 (2016). [PubMed: 27653704]
4. Jafari P, Braissant O, Zavadakova P, Henry H, Bonafe L, Ballhausen D, Brain damage in methylmalonic aciduria: 2-methylcitrate induces cerebral ammonium accumulation and apoptosis in 3D organotypic brain cell cultures. Orphanet J Rare Dis 8, 4 (2013). [PubMed: 23298464]

Author Manuscript Author Manuscript Author Manuscript Author Manuscript

5. Manoli I, Venditti CP, Disorders of branched chain amino acid metabolism. Transl Sci Rare Dis 1, 91–110 (2016). [PubMed: 29152456]
6. Molema F, Martinelli D, Horster F, Kolker S, Tangeraas T, de Koning B, Dionisi-Vici C, Williams M, additional ERN individual contributors of Metab, Liver and/or kidney transplantation in amino and organic acid-related inborn errors of metabolism: An overview on European data. J Inherit Metab Dis 44, 593–605 (2021). [PubMed: 32996606]
7. Baumgartner MR, Horster F, Dionisi-Vici C, Haliloglu G, Karall D, Chapman KA, Huemer M, Hochuli M, Assoun M, Ballhausen D, Burlina A, Fowler B, Grunert SC, Grunewald S, Honzik T, Merinero B, Perez-Cerda C, Scholl-Burgi S, Skovby F, Wijburg F, MacDonald A, Martinelli D, Sass JO, Valayannopoulos V, Chakrapani A, Proposed guidelines for the diagnosis and management of methylmalonic and propionic acidemia. Orphanet J Rare Dis 9, 130 (2014). [PubMed: 25205257]
8. Cosson MA, Benoist JF, Touati G, Dechaux M, Royer N, Grandin L, Jais JP, Boddaert N, Barbier V, Desguerre I, Campeau PM, Rabier D, Valayannopoulos V, Niaudet P, de Lonlay P, Long-term outcome in methylmalonic aciduria: a series of 30 French patients. Mol Genet Metab 97, 172–178 (2009). [PubMed: 19375370]
9. Nagarajan S, Enns GM, Millan MT, Winter S, Sarwal MM, Management of methylmalonic acidaemia by combined liver-kidney transplantation. J Inherit Metab Dis 28, 517–524 (2005). [PubMed: 15902554]
10. Mc Guire PJ, Lim-Melia E, Diaz GA, Raymond K, Larkin A, Wasserstein MP, Sansaricq C, Combined liver-kidney transplant for the management of methylmalonic aciduria: a case report and review of the literature. Mol Genet Metab 93, 22–29 (2008). [PubMed: 17964841]
11. Niemi AK, Kim IK, Krueger CE, Cowan TM, Baugh N, Farrell R, Bonham CA, Concepcion W, Esquivel CO, Enns GM, Treatment of methylmalonic acidemia by liver or combined liver-kidney transplantation. J Pediatr 166, 1455–1461 e1451 (2015). [PubMed: 25771389]
12. van ‘t Hoff WG, Dixon M, Taylor J, Mistry P, Rolles K, Rees L, Leonard JV, Combined liver-kidney transplantation in methylmalonic acidemia. J Pediatr 132, 1043–1044 (1998). [PubMed: 9627602]
13. Sakamoto R, Nakamura K, Kido J, Matsumoto S, Mitsubuchi H, Inomata Y, Endo F, Improvement in the prognosis and development of patients with methylmalonic acidemia after living donor liver transplant. Pediatr Transplant 20, 1081–1086 (2016). [PubMed: 27670840]
14. Collado MS, Armstrong AJ, Olson M, Hoang SA, Day N, Summar M, Chapman KA, Reardon J, Figler RA, Wamhoff BR, Biochemical and anaplerotic applications of in vitro models of propionic acidemia and methylmalonic acidemia using patient-derived primary hepatocytes. Mol Genet Metab 130, 183–196 (2020). [PubMed: 32451238]
15. Bowman CE, Wolfgang MJ, Role of the malonyl-CoA synthetase ACSF3 in mitochondrial metabolism. Adv Biol Regul 71, 34–40 (2019). [PubMed: 30201289]
16. Bowman CE, Rodriguez S, Alpergin ESS, Acoba MG, Zhao L, Hartung T, Claypool SM, Watkins PA, Wolfgang MJ, The Mammalian Malonyl-CoA Synthetase ACSF3 Is Required for Mitochondrial Protein Malonylation and Metabolic Efficiency. Cell Chem Biol 24, 673−+ (2017). [PubMed: 28479296]
17. Sloan JL, Johnston JJ, Manoli I, Chandler RJ, Krause C, Carrillo-Carrasco N, Chandrasekaran SD, Sysol JR, O’Brien K, Hauser NS, Sapp JC, Dorward HM, Huizing M, Group NIHISC, Barshop BA, Berry SA, James PM, Champaigne NL, de Lonlay P, Valayannopoulos V, Geschwind MD, Gavrilov DK, Nyhan WL, Biesecker LG, Venditti CP, Exome sequencing identifies ACSF3 as a cause of combined malonic and methylmalonic aciduria. Nat Genet 43, 883–886 (2011). [PubMed: 21841779]
18. Carrico C, Meyer JG, He W, Gibson BW, Verdin E, The Mitochondrial Acylome Emerges: Proteomics, Regulation by Sirtuins, and Metabolic and Disease Implications. Cell Metab 27, 497–512 (2018). [PubMed: 29514063]
19. Walsh C, Posttranslational Modification of Proteins: Expanding Nature’s Inventory. (Ben Roberts, 2006).
20. Yang XJ, Seto E, Lysine acetylation: codified crosstalk with other posttranslational modifications. Mol Cell 31, 449–461 (2008). [PubMed: 18722172]

Author Manuscript Author Manuscript Author Manuscript Author Manuscript

21. Glozak MA, Sengupta N, Zhang X, Seto E, Acetylation and deacetylation of non-histone proteins. Gene 363, 15–23 (2005). [PubMed: 16289629]
22. Ngounou Wetie AG, Woods AG, Darie CC, Mass spectrometric analysis of post-translational modifications (PTMs) and protein-protein interactions (PPIs). Adv Exp Med Biol 806, 205–235 (2014). [PubMed: 24952184]
23. Wagner GR, Payne RM, Widespread and enzyme-independent Nepsilon-acetylation and Nepsilon-succinylation of proteins in the chemical conditions of the mitochondrial matrix. J Biol Chem 288, 29036–29045 (2013). [PubMed: 23946487]
24. Cheng Z, Tang Y, Chen Y, Kim S, Liu H, Li SS, Gu W, Zhao Y, Molecular characterization of propionyllysines in non-histone proteins. Mol Cell Proteomics 8, 45–52 (2009). [PubMed: 18753126]
25. Chen Y, Sprung R, Tang Y, Ball H, Sangras B, Kim SC, Falck JR, Peng J, Gu W, Zhao Y, Lysine propionylation and butyrylation are novel post-translational modifications in histones. Mol Cell Proteomics 6, 812–819 (2007). [PubMed: 17267393]
26. Sterner DE, Berger SL, Acetylation of histones and transcription-related factors. Microbiol Mol Biol Rev 64, 435–459 (2000). [PubMed: 10839822]
27. Hirschey MD, Zhao Y, Metabolic Regulation by Lysine Malonylation, Succinylation, and Glutarylation. Mol Cell Proteomics 14, 2308–2315 (2015). [PubMed: 25717114]
28. Kulkarni RA, Worth AJ, Zengeya TT, Shrimp JH, Garlick JM, Roberts AM, Montgomery DC, Sourbier C, Gibbs BK, Mesaros C, Tsai YC, Das S, Chan KC, Zhou M, Andresson T, Weissman AM, Linehan WM, Blair IA, Snyder NW, Meier JL, Discovering Targets of Non-enzymatic Acylation by Thioester Reactivity Profiling. Cell Chem Biol 24, 231–242 (2017). [PubMed: 28163016]
29. Pougovkina O, te Brinke H, Wanders RJA, Houten SM, de Boer VCJ, Aberrant protein acylation is a common observation in inborn errors of acyl-CoA metabolism. Journal of Inherited Metabolic Disease 37, 709–714 (2014). [PubMed: 24531926]
30. Zhao SM, Xu W, Jiang WQ, Yu W, Lin Y, Zhang TF, Yao J, Zhou L, Zeng YX, Li H, Li YX, Shi J, An WL, Hancock SM, He FC, Qin LX, Chin J, Yang PY, Chen X, Lei QY, Xiong Y, Guan KL, Regulation of Cellular Metabolism by Protein Lysine Acetylation. Science 327, 1000–1004 (2010). [PubMed: 20167786]
31. Wagner GR, Bhatt DP, O'Connell TM, Thompson JW, Dubois LG, Backos DS, Yang H, Mitchell GA, Ilkayeva OR, Stevens RD, Grimsrud PA, Hirschey MD, A Class of Reactive Acyl-CoA Species Reveals the Non-enzymatic Origins of Protein Acylation. Cell Metab 25, 823–837 e828 (2017). [PubMed: 28380375]
32. Manoli I, Sysol JR, Epping MW, Li L, Wang C, Sloan JL, Pass A, Gagne J, Ktena YP, Li L, Trivedi NS, Ouattara B, Zerfas PM, Hoffmann V, Abu-Asab M, Tsokos MG, Kleiner DE, Garone C, Cusmano-Ozog K, Enns GM, Vernon HJ, Andersson HC, Grunewald S, Elkahloun AG, Girard CL, Schnermann J, DiMauro S, Andres-Mateos E, Vandenberghe LH, Chandler RJ, Venditti CP, FGF21 underlies a hormetic response to metabolic stress in methylmalonic acidemia. JCI Insight 3, (2018).
33. Crane AM, Martin LS, Valle D, Ledley FD, Phenotype of disease in three patients with identical mutations in methylmalonyl CoA mutase. Hum Genet 89, 259–264 (1992). [PubMed: 1351030]
34. Froese DS, Fowler B, Baumgartner MR, Vitamin B12 , folate, and the methionine remethylation cycle-biochemistry, pathways, and regulation. J Inherit Metab Dis 42, 673–685 (2019). [PubMed: 30693532]
35. Epping MW, Wang CX, Manoli I, Fraser JL, Gomez-Rodriguez J, Elliot G, Sloan JL, Hoffmann V, Schwartzberg PL, Venditti CP . (The 65th Annual Meeting of the American Society of Human Genetics , Baltimore, MD, USA, 2015).
36. Verdin E, Hirschey MD, Finley LW, Haigis MC, Sirtuin regulation of mitochondria: energy production, apoptosis, and signaling. Trends Biochem Sci 35, 669–675 (2010). [PubMed: 20863707]
37. Park J, Chen Y, Tishkoff DX, Peng C, Tan MJ, Dai LZ, Xie ZY, Zhang Y, Zwaans BMM, Skinner ME, Lombard DB, Zhao YM, SIRT5-Mediated Lysine Desuccinylation Impacts Diverse Metabolic Pathways. Molecular Cell 50, 919–930 (2013). [PubMed: 23806337]

Author Manuscript Author Manuscript Author Manuscript Author Manuscript

38. Rardin MJ, He WJ, Nishida Y, Newman JC, Carrico C, Danielson SR, Guo A, Gut P, Sahu AK, Li B, Uppala R, Fitch M, Riiff T, Zhu L, Zhou J, Mulhern D, Stevens RD, Ilkayeva OR, Newgard CB, Jacobson MP, Hellerstein M, Goetzman ES, Gibson BW, Verdin E, SIRT5 Regulates the Mitochondrial Lysine Succinylome and Metabolic Networks. Cell Metabolism 18, 920–933 (2013). [PubMed: 24315375]

39. Nakagawa T, Lomb DJ, Haigis MC, Guarente L, SIRT5 Deacetylates carbamoyl phosphate synthetase 1 and regulates the urea cycle. Cell 137, 560–570 (2009). [PubMed: 19410549]

40. Hada K, Hirota K, Inanobe A, Kako K, Miyata M, Araoi S, Matsumoto M, Ohta R, Arisawa M, Daitoku H, Hanada T, Fukamizu A, Tricarboxylic acid cycle activity suppresses acetylation of mitochondrial proteins during early embryonic development in Caenorhabditis elegans. J Biol Chem 294, 3091–3099 (2019). [PubMed: 30606736]

41. Tan M, Peng C, Anderson KA, Chhoy P, Xie Z, Dai L, Park J, Chen Y, Huang H, Zhang Y, Ro J, Wagner GR, Green MF, Madsen AS, Schmiesing J, Peterson BS, Xu G, Ilkayeva OR, Muehlbauer MJ, Braulke T, Muhlhausen C, Backos DS, Olsen CA, McGuire PJ, Pletcher SD, Lombard DB, Hirschey MD, Zhao Y, Lysine glutarylation is a protein posttranslational modification regulated by SIRT5. Cell Metab 19, 605–617 (2014). [PubMed: 24703693]

42. Wagner GR, Hirschey MD, Nonenzymatic protein acylation as a carbon stress regulated by sirtuin deacylases. Mol Cell 54, 5–16 (2014). [PubMed: 24725594]

43. Huang da W, Sherman BT, Lempicki RA, Systematic and integrative analysis of large gene lists using DAVID bioinformatics resources. Nat Protoc 4, 44–57 (2009). [PubMed: 19131956]

44. Huang da W, Sherman BT, Lempicki RA, Bioinformatics enrichment tools: paths toward the comprehensive functional analysis of large gene lists. Nucleic Acids Res 37, 1–13 (2009). [PubMed: 19033363]

45. Zhou G, Soufan O, Ewald J, Hancock REW, Basu N, Xia J, NetworkAnalyst 3.0: a visual analytics platform for comprehensive gene expression profiling and meta-analysis. Nucleic Acids Res 47, W234–W241 (2019). [PubMed: 30931480]

46. Xia J, Gill EE, Hancock RE, NetworkAnalyst for statistical, visual and network-based meta-analysis of gene expression data. Nat Protoc 10, 823–844 (2015). [PubMed: 25950236]

47. Xia J, Benner MJ, Hancock RE, NetworkAnalyst--integrative approaches for protein-protein interaction network analysis and visual exploration. Nucleic Acids Res 42, W167–174 (2014). [PubMed: 24861621]

48. Xia J, Lyle NH, Mayer ML, Pena OM, Hancock RE, INVEX--a web-based tool for integrative visualization of expression data. Bioinformatics 29, 3232–3234 (2013). [PubMed: 24078684]

49. Xia J, Fjell CD, Mayer ML, Pena OM, Wishart DS, Hancock RE, INMEX--a web-based tool for integrative meta-analysis of expression data. Nucleic Acids Res 41, W63–70 (2013). [PubMed: 23766290]

50. Du JT, Zhou YY, Su XY, Yu JJ, Khan S, Jiang H, Kim J, Woo J, Kim JH, Choi BH, He B, Chen W, Zhang S, Cerione RA, Auwerx J, Hao Q, Lin HN, Sirt5 Is a NAD-Dependent Protein Lysine Demalonylase and Desuccinylase. Science 334, 806–809 (2011). [PubMed: 22076378]

51. Pierson DL, A rapid colorimetric assay for carbamyl phosphate synthetase I. J Biochem Biophys Methods 3, 31–37 (1980). [PubMed: 7451805]

52. Amaral AU, Cecatto C, Castilho RF, Wajner M, 2-Methylcitric acid impairs glutamate metabolism and induces permeability transition in brain mitochondria. J Neurochem 137, 62–75 (2016). [PubMed: 26800654]

53. Aleshin VA, Mkrtchyan GV, Kaehne T, Graf AV, Maslova MV, Bunik VI, Diurnal regulation of the function of the rat brain glutamate dehydrogenase by acetylation and its dependence on thiamine administration. J Neurochem 153, 80–102 (2020). [PubMed: 31886885]

54. Caterino M, Chandler RJ, Sloan JL, Dorko K, Cusmano-Ozog K, Ingenito L, Strom SC, Imperlini E, Scolamiero E, Venditti CP, Ruoppolo M, The proteome of methylmalonic acidemia (MMA): the elucidation of altered pathways in patient livers. Mol Biosyst 12, 566–574 (2016). [PubMed: 26672496]

55. King GA, Hashemi Shabestari M, Taris KH, Pandey AK, Venkatesh S, Thilagavathi J, Singh K, Krishna Koppisetti R, Temiakov D, Roos WH, Suzuki CK, Wuite GJL, Acetylation and

Author Manuscript Author Manuscript Author Manuscript Author Manuscript

phosphorylation of human TFAM regulate TFAM-DNA interactions via contrasting mechanisms. Nucleic Acids Res 46, 3633–3642 (2018). [PubMed: 29897602]

56. Minczuk M, He J, Duch AM, Ettema TJ, Chlebowski A, Dzionek K, Nijtmans LG, Huynen MA, Holt IJ, TEFM (c17orf42) is necessary for transcription of human mtDNA. Nucleic Acids Res 39, 4284–4299 (2011). [PubMed: 21278163]
57. Chandler RJ, Zerfas PM, Shanske S, Sloan J, Hoffmann V, DiMauro S, Venditti CP, Mitochondrial dysfunction in mut methylmalonic acidemia. FASEB J 23, 1252–1261 (2009). [PubMed: 19088183]
58. Manoli I, Sysol JR, Li L, Houillier P, Garone C, Wang C, Zerfas PM, Cusmano-Ozog K, Young S, Trivedi NS, Cheng J, Sloan JL, Chandler RJ, Abu-Asab M, Tsokos M, Elkahloun AG, Rosen S, Enns GM, Berry GT, Hoffmann V, DiMauro S, Schnermann J, Venditti CP, Targeting proximal tubule mitochondrial dysfunction attenuates the renal disease of methylmalonic acidemia. Proc Natl Acad Sci U S A 110, 13552–13557 (2013). [PubMed: 23898205]
59. Luciani A, Denley MCS, Govers LP, Sorrentino V, Froese DS, Mitochondrial disease, mitophagy, and cellular distress in methylmalonic acidemia. Cell Mol Life Sci 78, 6851–6867 (2021). [PubMed: 34524466]
60. Childs B, Nyhan WL, Borden M, Bard L, Cooke RE, Idiopathic hyperglycinemia and hyperglycinuria: a new disorder of amino acid metabolism. I. Pediatrics 27, 522–538 (1961). [PubMed: 13693094]
61. Childs B, Nyhan WL, Further Observations of a Patient with Hyperglycinemia. Pediatrics 33, 403–412 (1964). [PubMed: 14129085]
62. Hommes FA, Kuipers JR, Elema JD, Jansen JF, Jonxis JH, Propionicacidemia, a new inborn error of metabolism. Pediatr Res 2, 519–524 (1968). [PubMed: 5727920]
63. Hsia YE, Scully KJ, Rosenberg LE, Defective propionate carboxylation in ketotic hyperglycinaemia. Lancet 1, 757–758 (1969). [PubMed: 4180220]
64. Endo H, Yoshida M, Hayashi F, Yokoyama S, Solution structure of the GCV_H domain from mouse glycine. (2007).
65. Hirschey MD, Shimazu T, Huang JY, Schwer B, Verdin E, SIRT3 regulates mitochondrial protein acetylation and intermediary metabolism. Cold Spring Harb Symp Quant Biol 76, 267–277 (2011). [PubMed: 22114326]
66. Shimazu T, Hirschey MD, Hua L, Dittenhafer-Reed KE, Schwer B, Lombard DB, Li Y, Bunkenborg J, Alt FW, Denu JM, Jacobson MP, Verdin E, SIRT3 deacetylates mitochondrial 3-hydroxy-3-methylglutaryl CoA synthase 2 and regulates ketone body production. Cell Metab 12, 654–661 (2010). [PubMed: 21109197]
67. Choi JE, Mostoslavsky R, Sirtuins, metabolism, and DNA repair. Curr Opin Genet Dev 26, 24–32 (2014). [PubMed: 25005742]
68. Schneller JL, Lee CM, Chandler RJ, Venturoni LE, Li A, Myung S, Cradick TJ, Hurley AE, Lagor WR, Bao G, Venditti CP, In Vivo Genome Editing at the Albumin Locus to TreatMethylmalonic Acidemia (MMA). Molecular Therapy-Methods and Clinical Development, (2021).
69. Lombard DB, Alt FW, Cheng HL, Bunkenborg J, Streeper RS, Mostoslavsky R, Kim J, Yancopoulos G, Valenzuela D, Murphy A, Yang Y, Chen Y, Hirschey MD, Bronson RT, Haigis M, Guarente LP, Farese RV Jr., Weissman S, Verdin E, Schwer B, Mammalian Sir2 homolog SIRT3 regulates global mitochondrial lysine acetylation. Mol Cell Biol 27, 8807–8814 (2007). [PubMed: 17923681]
70. Sanderson S, Green A, Preece MA, Burton H, The incidence of inherited metabolic disorders in the West Midlands, UK. Arch Dis Child 91, 896–899 (2006). [PubMed: 16690699]
71. Gueant JL, Gueant-Rodriguez RM, Kosgei VJ, Coelho D, Causes and consequences of impaired methionine synthase activity in acquired and inherited disorders of vitamin B12 metabolism. Crit Rev Biochem Mol Biol, 1–23 (2021).
72. Wu J, Liu J, Lapenta K, Desrouleaux R, Li MD, Yang X, Regulation of the urea cycle by CPS1 O-GlcNAcylation in response to dietary restriction and aging. J Mol Cell Biol, (2022).
73. Wang S, Osgood AO, Chatterjee A, Uncovering post-translational modification-associated protein-protein interactions. Curr Opin Struct Biol 74, 102352 (2022). [PubMed: 35334254]

Author Manuscript Author Manuscript Author Manuscript Author Manuscript

74. Johnson M, Zaretskaya I, Raytselis Y, Merezhuk Y, McGinnis S, Madden TL, NCBI BLAST: a better web interface. Nucleic Acids Res 36, W5–9 (2008). [PubMed: 18440982]

75. Hornbeck PV, Zhang B, Murray B, Kornhauser JM, Latham V, Skrzypek E, PhosphoSitePlus, 2014: mutations, PTMs and recalibrations. Nucleic Acids Res 43, D512–520 (2015). [PubMed: 25514926]

76. Adzhubei IA, Schmidt S, Peshkin L, Ramensky VE, Gerasimova A, Bork P, Kondrashov AS, Sunyaev SR, A method and server for predicting damaging missense mutations. Nat Methods 7, 248–249 (2010). [PubMed: 20354512]

77. Wang S HL.; Yu Z; Wu C; Cheng L; Wang Y; Chen K; Zhou S; Chen Q; Yu Y; and Li G , Interactions between sirtuins and fluorogenic small-molecule substrates offer insights into inhibitor design. RSC Advances, (2017).

78. Crooks GE, Hon G, Chandonia JM, Brenner SE, WebLogo: a sequence logo generator. Genome Res 14, 1188–1190 (2004). [PubMed: 15173120]

79. Schneider TD, Stephens RM, Sequence logos: a new way to display consensus sequences. Nucleic Acids Res 18, 6097–6100 (1990). [PubMed: 2172928]

80. Chandler RJ, Venditti CP, Long-term rescue of a lethal murine model of methylmalonic acidemia using adeno-associated viral gene therapy. Mol Ther 18, 11–16 (2010). [PubMed: 19861951]

81. Gao GP, Alvira MR, Wang L, Calcedo R, Johnston J, Wilson JM, Novel adeno-associated viruses from rhesus monkeys as vectors for human gene therapy. Proc Natl Acad Sci U S A 99, 11854–11859 (2002). [PubMed: 12192090]

Author Manuscript Author Manuscript Author Manuscript Author Manuscript

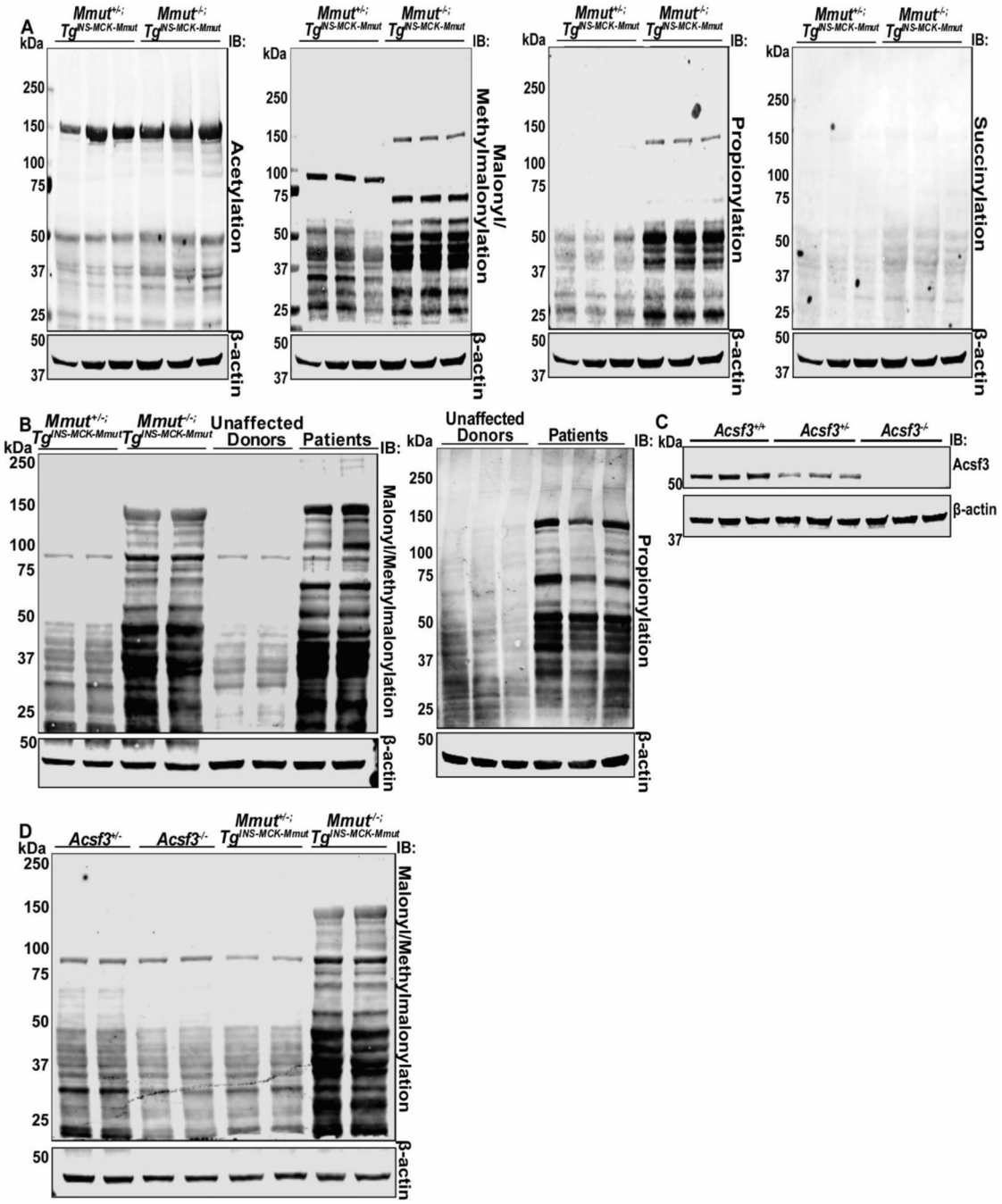

Figure 1. Malonylation/methylmalonylation and propionylation PTMs are elevated in murine MMA hepatic tissues.

A. Western blot analysis showing of hepatic tissues from *Mmut*$^{-/-}$;*Tg*$^{INS\text{-}MCK\text{-}Mmut}$ and *Mmut*$^{+/-}$;*Tg*$^{INS\text{-}MCK\text{-}Mmut}$ littermate controls. Blots were immunoblotted (IB) for acetylation, malonylation/methylmaonylation, propionylation, succinylation, and β-actin. β-actin served as a loading control. **B**. Western blot analysis of of liver tissue samples from patients with MMA and unaffected donors. Blots were immunoblotted for propionylation, malonylation/methylmalonylation, and β-actin. β-actin served as a loading control. **C.**

Author Manuscript Author Manuscript Author Manuscript Author Manuscript

Western blots of in murine hepatic tissues from *Acsf3*$^{-/-}$,*Acsf3*$^{+/-}$, and *Acsf3*$^{+/+}$ mice. Blots were immunoblotted for ACSF3 and β-actin. β-actin served as a loading control. **D.** Western blot analysis of hepatic tissues from *Acsf3*$^{-/-}$, *Acsf3*$^{+/-}$, *Mmut*$^{-/-}$;*Tg*$^{INS\text{-}MCK\text{-}Mmut}$, and *Mmut*$^{+/-}$;*Tg*$^{INS\text{-}MCK\text{-}Mmut}$ mice. . Blots were immunoblotted for propionylation, malonylation/methylmalonylation, and β-actin. β-actin served as a loading control.

Author Manuscript Author Manuscript Author Manuscript Author Manuscript

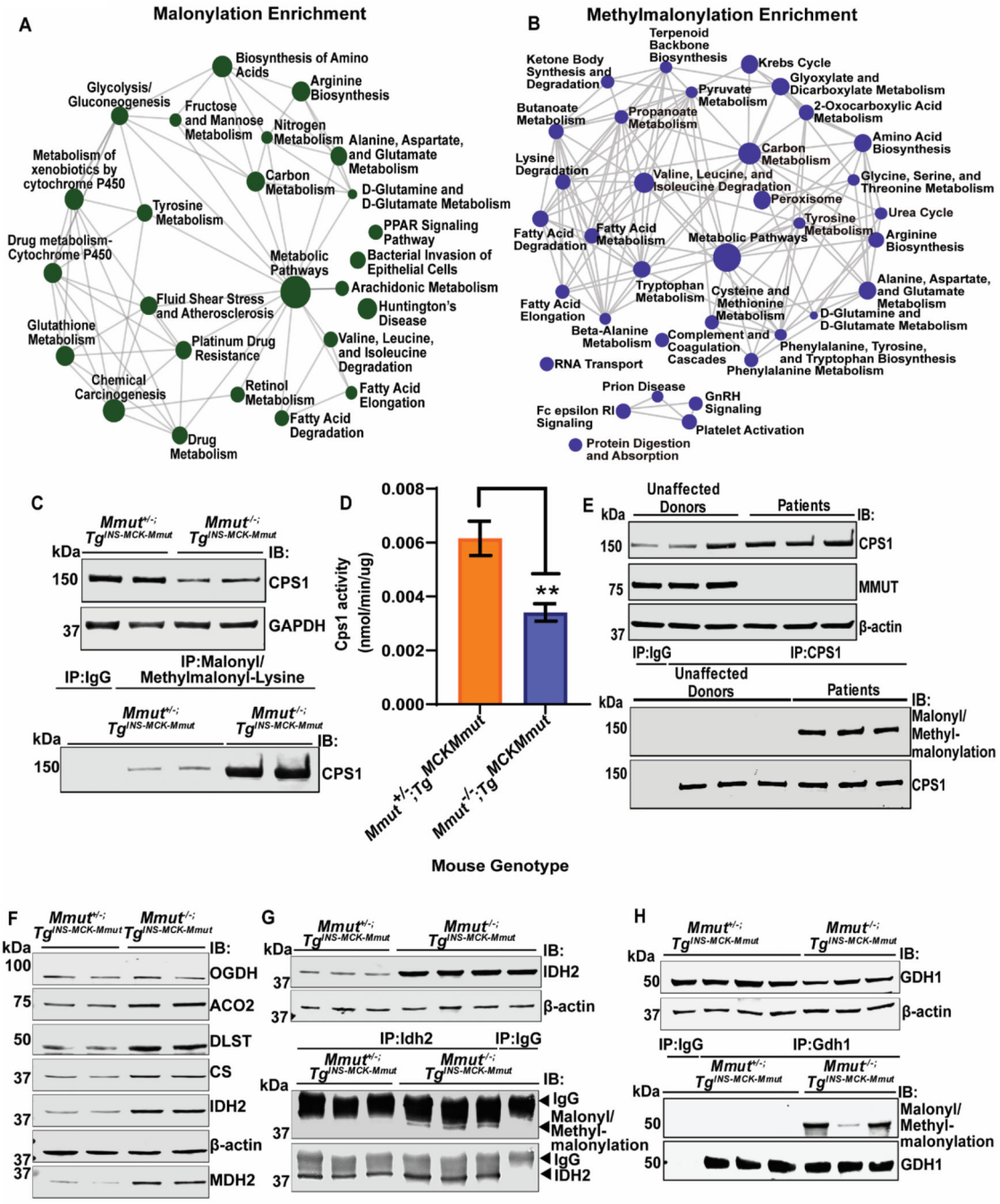

Figure 2. Mass spectrometry analysis and validation of the malonyl and methylmalonyl PTM proteome in MMA.

(A-B) Representation of cellular pathways containing proteins that were found to be aberrantly malonylated (A) or aberrantly methylmalonlated (**B**) in *Mmut*$^{-/-}$;*Tg*$^{INS\text{-}MCK\text{-}Mmut}$ mouse hepatic tissue compared to littermate controls as found by tandem mass spectrometry and gene ontology analysis. The size of each sphere is representative of the number of proteins modified in that pathway. **C.** Immunoprecipitation assay using an anti-malonylation antibody with cross-reactivity to methylmalonylation on hepatic tissue protein extracts

Author Manuscript Author Manuscript Author Manuscript Author Manuscript

from *Mmut*$^{-/-}$;*Tg*$^{INS\text{-}MCK\text{-}Mmut}$ mice and control *Mmut*$^{+/-}$;*Tg*$^{INS\text{-}MCK\text{-}Mmut}$ mice along with corresponding rabbit or mouse IgG immunoprecipitation. Immunoprecipitations were run on SDSPAGE analysis and were immunoblotted for CPS1. Corresponding input Western blot analysis for CPS1 and loading control Gapdh also shown. **D.** Enzymatic activity for CPS1 from livers of *Mmut*$^{-/-}$;*Tg*$^{INS\text{-}MCK\text{-}Mmut}$ mice (n=3) and control *Mmut*$^{+/-}$;*Tg*$^{INS\text{-}MCK\text{-}Mmut}$ mice (n=3). Each biological replicate was performed in technical triplicate. **E.** Immunoprecipitation assay using anti-CPS1 antibody on liver tissue protein extracts from patients with MMA and control liver tissue extracts along with corresponding rabbit or mouse IgG immunoprecipitation. We immunostained for malonyl/methylmalonylation and CPS1. Corresponding input Western blot analysis for CPS1, MMUT, and β-actin. **F.** Western blot analysis of total protein of Krebs cycle enzymes OGDH, ACO2, DLST, CS, IDH2, and MDH2 in hepatic tissue protein extracts from *Mmut*$^{-/-}$;*Tg*$^{INS\text{-}MCK\text{-}Mmut}$ mice and control *Mmut*$^{+/-}$;*Tg*$^{INS\text{-}MCK\text{-}Mmut}$ mice. **G.** Immunoprecipitation assay using anti-IDH2 antibody on hepatic tissue protein extracts from *Mmut*$^{-/-}$;*Tg*$^{INS\text{-}MCK\text{-}Mmut}$ mice and control *Mmut*$^{+/-}$;*Tg*$^{INS\text{-}MCK\text{-}Mmut}$ mice along with corresponding rabbit or mouse IgG immunoprecipitation followed by immunostaining for malonylation/methylmalonylation and IDH2. Corresponding input Western blot analysis for IDH2 and β-actin (loading control) can be found above. **H**. Immunoprecipitation assay using anti-GDH1 antibody on hepatic tissue protein extracts from *Mmut*$^{-/-}$;*Tg*$^{INS\text{-}MCK\text{-}Mmut}$ mice and control *Mmut*$^{+/-}$;*Tg*$^{INS\text{-}MCK\text{-}Mmut}$ mice along with corresponding rabbit or mouse IgG immunoprecipitation followed by immunostaining and Western blot analysis for malonylation/methylmalonylation and GDH1. Corresponding input Western blot analysis for GDH11 and β-actin (loading control) can be found above.

Author Manuscript Author Manuscript Author Manuscript Author Manuscript

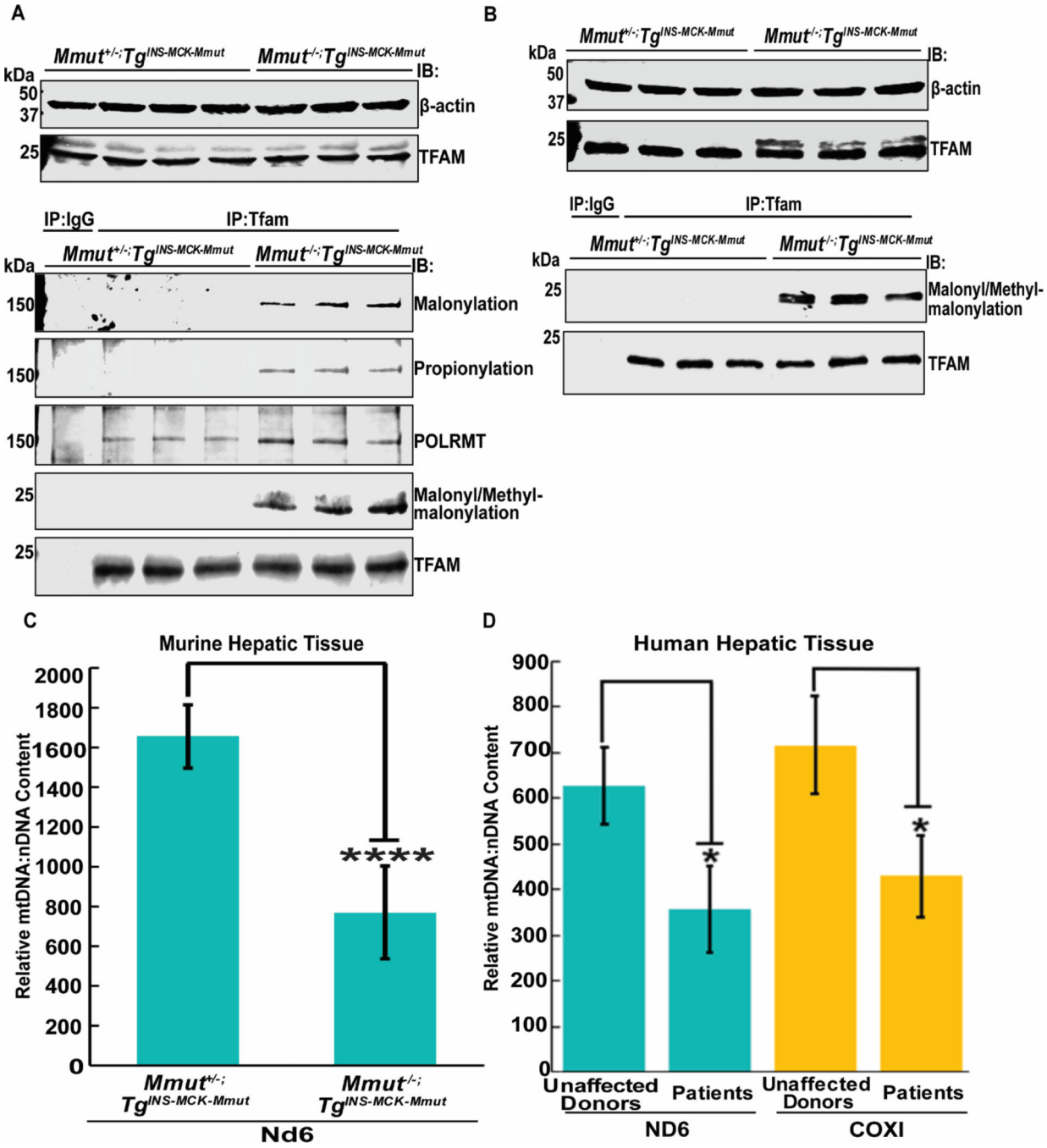

Figure 3. Aberrant acylation effects on mitochondrial DNA maintenance.

(A-B). Immunoprecipitation assay using anti-TFAM antibody on hepatic (**A**) and renal (**B**) tissue protein extracts from *Mmut*$^{-/-}$;*Tg*$^{INS\text{-}MCK\text{-}Mmut}$ mice and control *Mmut*$^{+/-}$;*Tg*$^{INS\text{-}MCK\text{-}Mmut}$ mice along with corresponding rabbit or mouse IgG immunoprecipitation. Resulting Western blots were immunoblotted for malonylation/ methylmalonylation, propionylation, POLRMT and TFAM. Corresponding input Western blot analysis for TFAM and β-actin (loading control) also shown. **C.** RT-PCR analysis of mitochondrial DNA copy number using probes against Nd6 in *Mmut*$^{-/-}$;*Tg*$^{INS\text{-}MCK\text{-}Mmut}$

Author Manuscript Author Manuscript Author Manuscript Author Manuscript

(n=3) mouse liver tissues as compared to *Mmut*$^{+/-}$;*Tg*$^{INS\text{-}MCK\text{-}Mmut}$ control mice (n=3). Mitochondrial DNA content was normalized to nuclear DNA using probes against β-actin. Each sample measurement was performed in technical duplicate. **D.** RT-PCR analysis of mitochondrial DNA copy number using probes against ND6 and COXI in liver tissues from patients with MMA (n=3) as compared to control human liver tissues (n=3). Mitochondrial DNA content was normalized to nuclear DNA using probes against β-actin. Each sample measurement was performed in technical duplicate.

Author Manuscript Author Manuscript Author Manuscript Author Manuscript

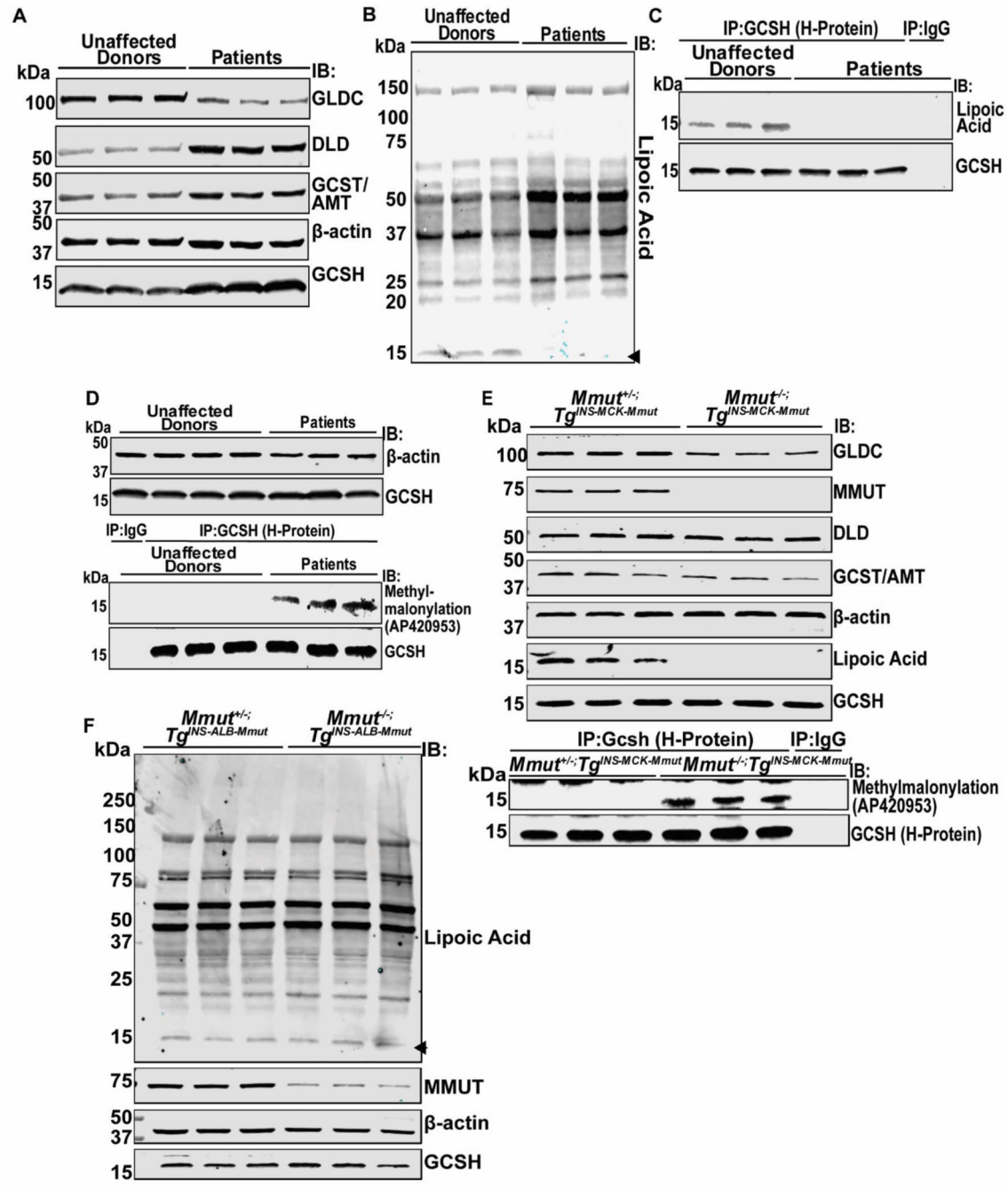

Figure 4. Aberrant acylation blocks lipoylation of H-Protein in the glycine cleavage system.

A. Western blot assay demostrating total GLDC, DLD, GCST/AMT and GCSH in hepatic tissues from patients with MMA and unaffected donor samples. β-actin served as loading control. **B.** Western blot assay demonstrating total lipoylation in hepatic tissues from patients with MMA and unaffected donor using the same samples and loading conditions as Figure 5A. **C.** Immunoprecipitation assay using anti-GCSH antibody on hepatic tissue protein extracts from patients with MMA and unaffected donors along with corresponding rabbit or mouse IgG immunoprecipitation followed by immunostaining for lipoylation

Author Manuscript Author Manuscript Author Manuscript Author Manuscript

and GCSH. Corresponding input Western blot analysis for GCSH and β-actin (loading control) are shown in (B). Excess protein lysate from patient sample 3 was used for IgG control immunoprecipitation. **D.** Immunoprecipitation assay using anti-GCSH antibody on hepatic tissue protein extracts from patients with MMA and unaffected donors along with corresponding rabbit or mouse IgG immunoprecipitation followed by immunostaining for methylmalonylation and GCSH. Corresponding input Western blot analysis for GCSH and β-actin (loading control) also shown. **E.**.. Immunoprecipitation assay using anti-GCSH antibody on hepatic tissue protein extracts from $Mmut^{-/-};Tg^{INS\text{-}MCK\text{-}Mmut}$ mice and control $Mmut^{+/-};Tg^{INS\text{-}MCK\text{-}Mmut}$ mice along with rabbit or mouse IgG immunoprecipitation followed by immunostaining for methylmalonylation and GCSH. Corresponding input Western blot analysis for GLDC, DLD, GCST/AMT, MMUT, lipoylation, GCSH and β-actin (loading control) also shown. **F.** Western blot assay demonstrating total lipoylation, MMUT protein, β-actin (loading control) protein, and GCSH protein in in hepatic tissues from $Mmut^{+/-};Tg^{INS\text{-}MCK\text{-}Mmut}$ and $Mmut^{-/-};Tg^{INS\text{-}MCK\text{-}Mmut}$ mice. The arrow indicates the lipoylation PTM band corresponding to GCSH.

Author Manuscript Author Manuscript Author Manuscript Author Manuscript

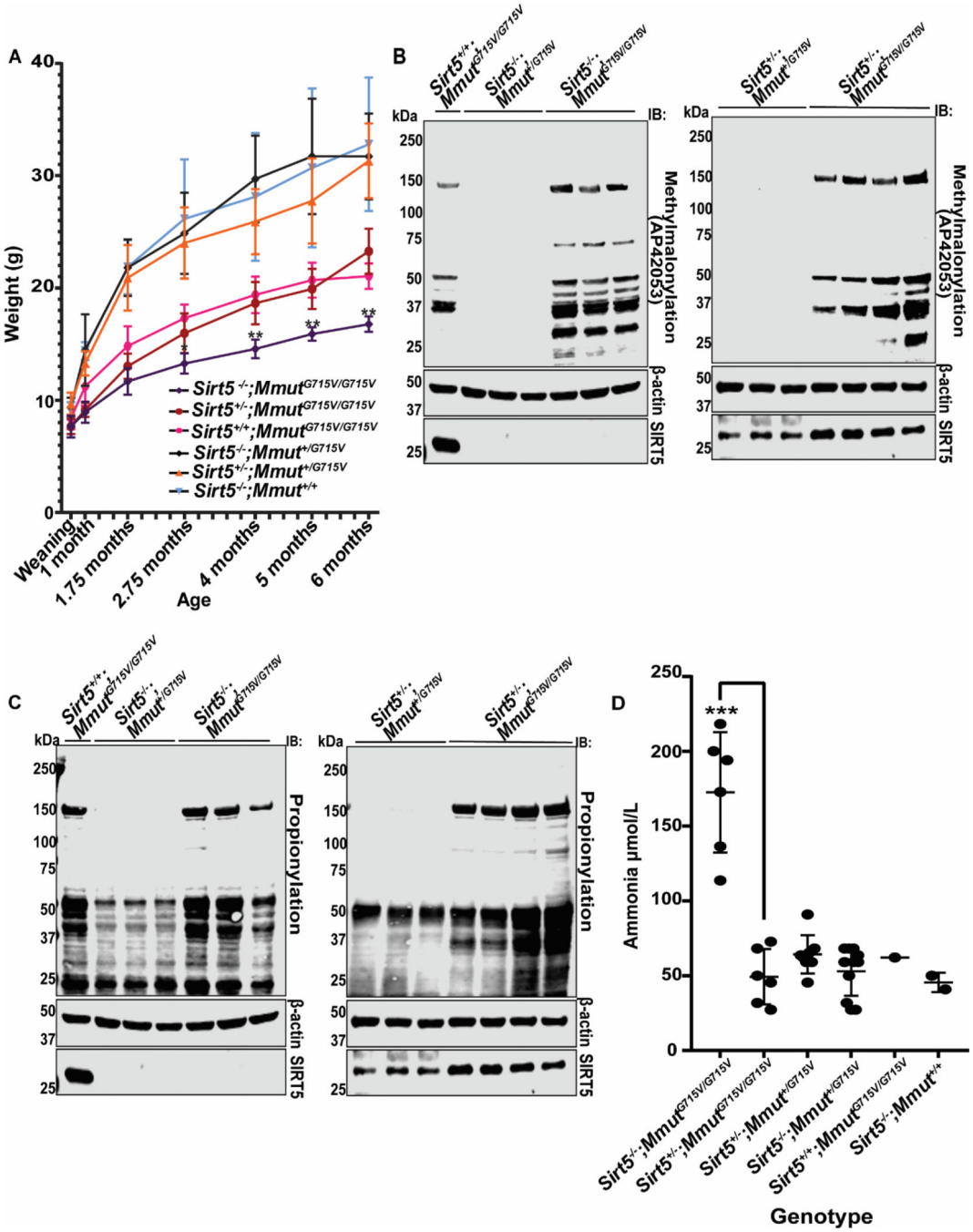

Figure 5. Loss of Sirt5 increases MMA disease severity in MmutG715V/G715V mice.

A. Weight data (g) of *Sirt5*$^{-/-}$;*Mmut*$^{G715V/G715V}$ mice (n=6, purple), *Sirt5*$^{+/-}$;*Mmut*$^{G715V/G715V}$ mice (n=6, red), *Sirt5*$^{+/+}$;*Mmut*$^{G715V/G715V}$ mice (n=4, pink), *Sirt5*$^{-/-}$;*Mmut*$^{+/G715V}$ mice (n=19, black), *Sirt5*$^{+/-}$;*Mmut*$^{+/G715V}$ mice (n=13, orange), and *Sirt5*$^{-/-}$;*Mmut*$^{+/+}$ mice (n=4, blue) from wean date to 6 months of age. (**p<0.01, **p=0.0048 at 4 months, **p=0.0028 at 5 months, and **p=0.0032 at 6 months) **B.** Western blot assay of hepatic tissue protein extract from *Sirt5*$^{+/+}$;*Mmut*$^{G715V/G715V}$ mice, *Sirt5*$^{-/-}$;*Mmut*$^{+/G715V}$ mice, *Sirt5*$^{-/-}$;*Mmut*$^{G715V/G715V}$

Author Manuscript Author Manuscript Author Manuscript Author Manuscript

mice, Sirt5$^{+/-}$;Mmut$^{+/G715V}$ mice, and *Sirt5*$^{+/-}$*;Mmut*$^{G715V/G715V}$ mice. Immunoblots were immunoblotted for methylmalonylation, Sirt5, and β-actin (loading control). **C.** Western blot assay of hepatic tissue protein extract from *Sirt5*$^{+/+}$*;Mmut*$^{G715V/G715V}$ mice, *Sirt5*$^{-/-}$*;Mmut*$^{+/G715V}$ mice *Sirt5*$^{-/-}$*;Mmut*$^{G715V/G715V}$ mice, *Sirt5*$^{+/-}$*;Mmut*$^{+/G715V}$ mice, and Sirt5$^{+/-}$;Mmut$^{G715V/G715V}$ mice. Immunoblots were immunoblotted for propionylation, Sirt5, and β-actin (loading control). D. Ammonia concentrations in terminal bleed plasma samples from *Sirt5−/−;MmutG715V/G715V* mice (n=6), *Sirt5*$^{+/-}$*;Mmut*$^{G715V/G715V}$ mice (n=6), *Sirt5*$^{+/-}$*;Mmut*$^{+/G715V}$ mice (n=8), *Sirt5*$^{-/-}$*;Mmut*$^{+/G715V}$ mice (n=11), *Sirt5*$^{+/+}$*;Mmut*$^{G715V/G715V}$ mice (n=1), and *Sirt5*$^{-/-}$*;Mmut*$^{+/+}$ mice (n=2) (***p<0.001, p=0.0002).

Author Manuscript Author Manuscript Author Manuscript Author Manuscript

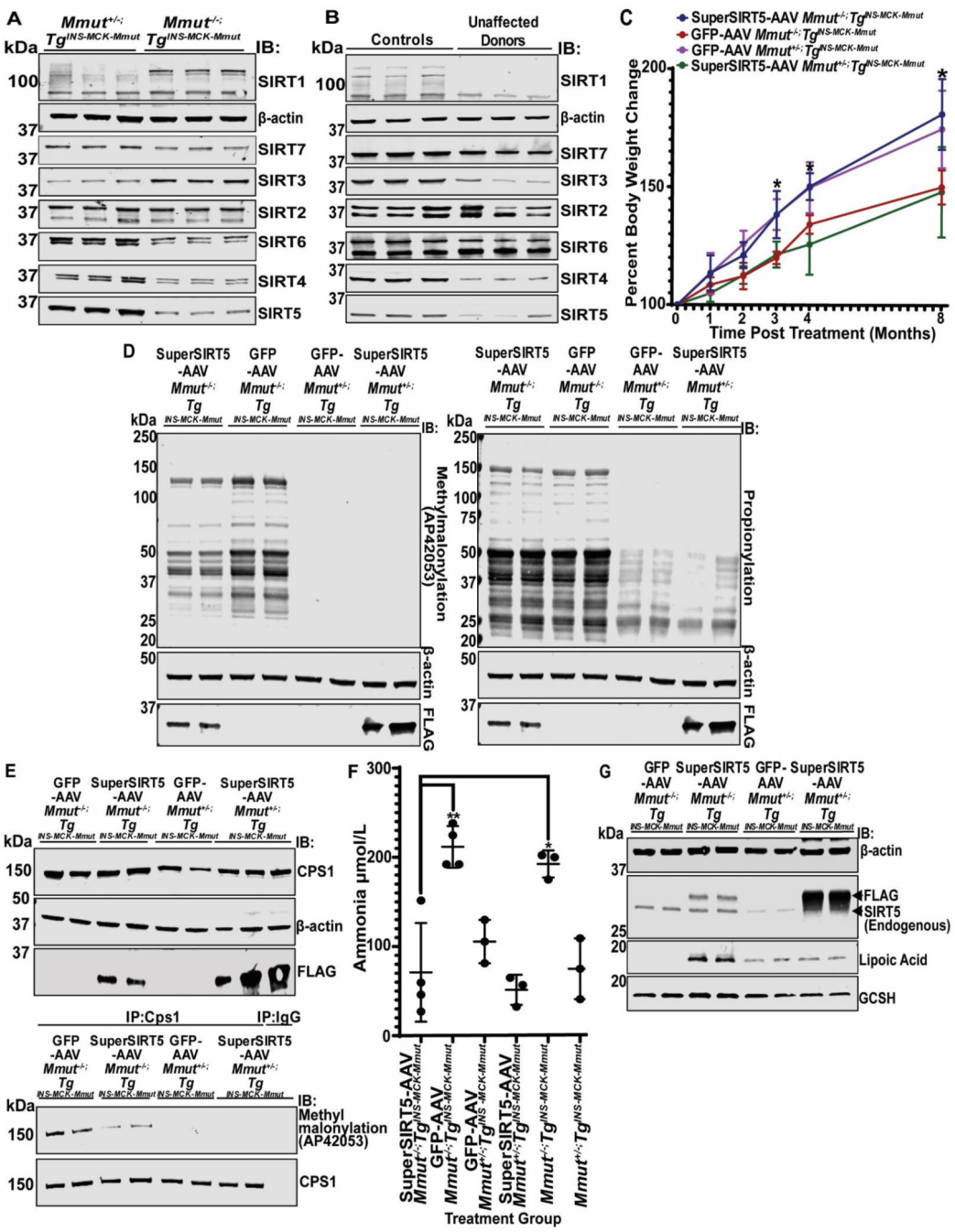

Figure 6. Acylation inhibition-resistant SIRT5 and its therapeutic application in an MMA mouse model.

A. Western blot assay of hepatic tissue protein extract from *Mmut*$^{-/-}$;*Tg*$^{INS\text{-}MCK\text{-}Mmut}$ and *Mmut*$^{+/-}$;*Tg*$^{INS\text{-}MCK\text{-}Mmut}$ immunoblotted for SIRT1, SIRT2, SIRT3, SIRT4, SIRT5, SIRT6, SIRT7, and β-actin (loading control). **B.** Western blot assay of hepatic tissue protein extract from patients with MMA and unaffected donors immunoblotted for SIRT1, SIRT2, SIRT3, SIRT4, SIRT5, SIRT6, SIRT7, and β-actin (loading control). **C.** Analysis of percent body weight change of *Mmut*$^{-/-}$;*Tg*$^{INS\text{-}MCK\text{-}Mmut}$ mice treated

Author Manuscript Author Manuscript Author Manuscript Author Manuscript

with SuperSIRT5-Flag AAV8 (n=4) or GFP AAV8 (n=5) and *Mmut*$^{+/-}$;*Tg*$^{INS\text{-}MCK\text{-}Mmut}$ mice treated with SuperSIRT5-Flag AAV8 (n=3) or GFP AAV8 (n=3) over 8 months after AAV injection. (*p<0.05, *p=0.039 at 3 months, *p=0.017 at 3 months, and *p=0.039 at 3 months) **D.** Western blot assay of hepatic tissue protein extract from *Mmut*$^{-/-}$;*Tg*$^{INS\text{-}MCK\text{-}Mmut}$ mice reated with SuperSIRT5-Flag AAV8 or GFP AAV8 and *Mmut*$^{+/-}$;*Tg*$^{INS\text{-}MCK\text{-}Mmut}$ mice treated with SuperSIRT5-Flag AAV8 or GFP AAV8. The resulting blots were immunoblotted for methylmalonylation, propionylation, Flag, and β-actin (loading control). **E.** Immunoprecipitation assay using anti-CPS1 antibody on hepatic tissue protein extracts from *Mmut*$^{-/-}$;*Tg*$^{INS\text{-}MCK\text{-}Mmut}$ mice treated with SuperSIRT5-Flag AAV8 or GFP AAV8 and control *Mmut*$^{+/-}$;*Tg*$^{INS\text{-}MCK\text{-}Mmut}$ mice treated with SuperSIRT5-Flag AAV8 or GFP AAV8 along with corresponding rabbit or mouse IgG immunoprecipitation followed by immunostaining for methylmalonylation and CPS1. Corresponding input Western blot analysis for CPS1, Flag, and β-actin (loading control) also shown. **F.** Ammonia assay performed on terminal bleed plasma samples from *Mmut*$^{-/-}$;*Tg*$^{INS\text{-}MCK\text{-}Mmut}$ mice treated with SuperSIRT5-Flag AAV8 (n=4) or GFP AAV8 (n=4), control *Mmut*$^{+/-}$;*Tg*$^{INS\text{-}MCK\text{-}Mmut}$ mice treated with SuperSIRT5-Flag AAV8 (n=3) or GFP AAV8 (n=3), and *Mmut*$^{-/-}$;*Tg*$^{INS\text{-}MCK\text{-}Mmut}$ (n=3) and *Mmut*$^{+/-}$;*Tg*$^{INS\text{-}MCK\text{-}Mmut}$ mice (n=3) that received no AAV treatment. (**p<0.01, **p=0.0092 and *p<0.05, *p=0.018) **G**. Western blot assay of hepatic tissue protein extract from *Mmut*$^{-/-}$;*Tg*$^{INS\text{-}MCK\text{-}Mmut}$ mice treated with SuperSIRT5-Flag AAV8 or GFP AAV8 and *Mmut*$^{+/-}$;*Tg*$^{INS\text{-}MCK\text{-}Mmut}$ mice treated with SuperSIRT5-Flag AAV8 or GFP AAV8. The resulting blot was immunoblotted for Sirt5, lipoylation, GCSH, and β-actin (loading control).